Investigation of Poultry Litter Biochar as a Potential Electrode for Direct Carbon Fuel Cell

By
Hamza Abdellaoui

Thesis submitted to the Faculty of the
Virginia Polytechnic Institute and State University
in partial fulfillment of the requirements for the degree of

MASTER OF SCIENCE
in
Biological Systems Engineering

Approved

Foster A. Agblevor, Chair

Mike Zhang, Co-Chair

Ryan Senger

Disapproved

Kamel Halouani

December 11, 2012

Blacksburg, Virginia

Keywords: poultry litter biochar, Direct Carbon Fuel Cell, demineralization, carbonization, electrical conductivity.

Investigation of Poultry Litter Biochar as a Potential Electrode for Direct Carbon Fuel Cell

By

Hamza Abdellaoui

Biological System Engineering/Fuel Processing Engineering

(ABSTRACT)

Direct carbon fuel cell (DCFC) is a high temperature fuel cell (around 700 °C) that produces electrical energy from the direct conversion of the chemical energy of carbon. DCFC has a higher achievable efficiency of 80% compared to other fuel cells and the corresponding CO_2 emission is very low compared to conventional coal-burning power plants. Moreover, a DCFC can use diversified fuel resources even waste material, which is advantageous compared to other types of fuel cells which are limited to specific fuels. DCFCs are still under development due to a number of fundamental and technological challenges such as the efficiency of carbon fuels and the effect of impurities on the performance and lifetime of the DCFC. These are key factors for the development and commercialization of these devices. In this study, three biochars obtained from the pyrolysis of poultry litters (PL) collected from Tunisian and US farmers, were characterized to see whether they can be potential anode fuels for DCFC or not. PL biochars have low fixed carbon contents (19-35 wt%) and high ash contents (32.5-63 wt%). These ashes contain around 40 wt% catalytic oxides for carbon oxidation reaction, however, these oxides have very low electrical conductivities, which resulted in the very low (negligible) electrical conductivity of the PL biochars ($7.7x10^{-9}$-$70.56x10^{-9}$ S/cm) at room temperature. Moreover, the high ash contents resulted in low surface areas (3.34-4.2 m^2/g). These findings disqualified PL biochar from being a potential anode fuel for DCFCs.

Chemical demineralization in the sequence HF/HCl followed by carbonization at 950° C of the PL biochars will result in higher fixed carbon content, higher surface area, and higher electrical conductivities. Moreover, the treated PL biochars would contain a potential catalyst (Calcium in the form of CaF_2) for carbon oxidation. All these criteria would qualify the treated PL biochars to be potential fuels for DCFC.

DEDICATION

I dedicate this potential research work to Abdellaoui family, for their unlimited support and encouragement. I also want to dedicate this work to my dear wife TATIANA DRUGOVA for her unconditional support, understanding and love. I shouldn’t also forget to thank all my lab mates for their encouragement and inspiring suggestions that helped me to elaborate this work.

ACKNOWLEDGEMENTS

I would like to thank my advisors, Dr. Foster A. Agblevor and Dr. Kamel Halouani for their guidance and advices during my Master of Science study. I would like also to thank both the Engineering School of Sfax and Virginia Tech for giving me the opportunity of developing my research work in the U.S.A. through the Fuel Processing Engineering program.

I would like also to thank Dr Mike Zhang and Dr. Ryan Senger for being a part of this program and for their model lectures which widened my knowledge in the Bio-processing engineering and Molecular biology.

I would like to thank my Tunisian committee, Dr. Sami Sayadi and Dr. Hafed Belghith, for their contribution on this special research program.

I thank Utah State University for welcoming me as a visiting scholar and for providing the necessary resources for my research work.

I would like also to thank Cache Valley Machine, for their efficient service and appreciation for my work.

This project was primarily supported by a grant from the US Department of State (#S-TS800-09-GR-204) entitled, Virginia Tech-National Engineering School of Sfax partnership: towards strengthening of higher education & research capacities for better serving the economic development priorities in Tunisia. This project was also partially supported by a fund from Virginia Tech (#425997). The grant was administered by the US Embassy at Tunis.

TABLE OF CONTENTS

LIST OF FIGURES

LIST OF TABLES

Chapter 1
Introduction

1.1 Background

The strict emission requirements adopted by several countries (mainly those who are generating high levels of pollutants, such as CO_2 and other greenhouse gases) have contributed to the quick development of energy technologies based on renewable energy sources.

World demand for electricity is directly related to humans increasing need for energy. Development of new energy generation technologies to satisfy those needs is increasing as well. Up to date, coal burning is one of the most common methods used to generate electricity. This method produces greenhouse gases especially CO_2, which is the major cause of global warming. In addition to CO_2 generation, some varieties of coal release significant quantities of sulfur dioxide, which leads to acid rain. Various other impurities in coal, such as mercury (which is highly toxic) are also released in the air. (Li, 2008; Gohlke et al., 2011).

Direct Carbon Fuel Cell (DCFC) holds promise of reducing the climate change impacts of using coal. Direct carbon fuel cell is a high temperature fuel cell (around 700 °C) that produces electricity from the conversion of a carbon rich material (anode) through combination of carbon with oxygen (cathode), and releases carbon dioxide as byproduct. The combination of carbon and oxygen occurs in an electrolyte. (Cao et al., 2007).

Scientists are investigating this device (DCFC) because of its higher achievable efficiency (80%) compared to conventional coal-burning power plants, and its fuel flexibility since it can convert any type of solid carbon from many different resources, including coal, petroleum coke, biomass (e.g., rice hulls, nut shells, corn husks, grass, and woods) and even organic garbage. Developments and improvements are still being made for DCFC to enhance its efficiency and to commercialize it (scale up) (Chen et al., 2010).

The DCFC technology provides a promising opportunity to improve the management of widely available residues and wastes (such as agricultural and organic industry wastes) and it is also a solution for common waste-disposal problems and reduction of air pollution.

Currently, the electrochemical reactivity of carbon materials as a potential fuel for DCFC has been investigated and tested. The performance of the DCFC is related to the availability (structure, wetting ability) of carbon particle for the oxidation reaction and the chemical properties (surface oxygen-containing groups) of the surface of those carbon materials. Therefore, the relationship between the physico-chemical characteristics of carbon fuels and their electrochemical reactivity in the DCFC can be investigated to determine the essential factors affecting the performance of the DCFC. (Cao et al., 2010; Li et al., 2009; Chen et al., 2010).

1.2 Research objectives

Poultry litter biochar has been used for agricultural applications (soil amendment, bulking agent, etc). The application of poultry litter biochar to generate electricity through electrochemical reactions at high temperature has not been reported. Thus the goal of this project is to investigate poultry litter biochar as a potential electrode/electrolyte for direct carbon fuel cells (DCFCs). The specific objectives are:

1. Characterization of the biochars obtained after pyrolysis of poultry litter collected from Tunisian and US farms, and compare them to the industrial carbons (Activated carbon, Carbon black and Graphite) discussed in the literature.

2. Determine whether poultry litter biochar can be considered as a potential electrode for DCFCs.

References

1. Cao, D., Wang, G., Wang, C., Wang, J., Lu, T. 2010. Enhancement of electrooxidation activity of activated carbon for direct carbon fuel cell. *International journal of hydrogen energy* 35: 1778–1782.

2. Gohlke, J. M., Thomas, R., Woodward, A., Campbell-Lendrum, D., Prüss-üstün, A., Hales, S., Portier, C. J. 2011. Estimating the global public health implications of electricity and coal consumption. *Environmental Health Perspectives* 119: 821 - 826.

3. Chen, M., Wang, C., Niu, X., Zhao, S., Tang, J., Zhu, B. 2010. Carbon anode in direct carbon fuel cell. *international journal of hydrogen energy* 35: 2732 – 2736.

4. Li, X., Zhu. Z., Chen, J., De Marco, R., Dicks, A., Bradley, J., Lu, G. 2009. Surface modification of carbon fuels for direct carbon fuel cells. *Journal of Power Sources.* 186: 1–9.

5. Li, X. 2008. Tailoring carbon materials as fuels for the direct carbon fuel cells. PhD thesis (University of Queensland, Australia).

Chapter 2
Literature review

2.1 Introduction

In this chapter, a literature review began with a brief historical definition of the DCFC, followed by a description of the different configurations and technologies of direct carbon fuel cells. Furthermore, the benefits of DCFC compared to other types of fuel cells, as well as the engineering challenges for the DCFC development are discussed. A second part of this literature review described the common carbon materials that were used in the literature as anode fuel for DCFC. A description of biochar as well as poultry litter biochar, and their production methods, was developed as the final part of this chapter.

2.2 Historical contest and Definition of the DCFC

Direct Carbon Fuel Cells (DCFC) were not a popular device for electricity generation since they started to be tested in the mid-19th century due to their low efficiency (8%) (Jacques, 1896) and instability (electrolyte and anode degradation) compared to the coal-burning electricity generation plants. However, factors such as constant increase in fossil-oil prices, greenhouse gas emissions and the sustainability of energy supply has led to DCFCs gaining more attention within the scientific and public community.

A DCFC (Figure 2.1) is a high temperature fuel cell (600 to 800° C) that converts the chemical energy in solid carbon directly into electricity through direct electrochemical oxidation. (Cao et al., 2007).

The overall reaction of the fuel cell is shown in Equation 2.1.

$$C\,(s) + O_2(g) = CO_2(g) \qquad (2.1)$$

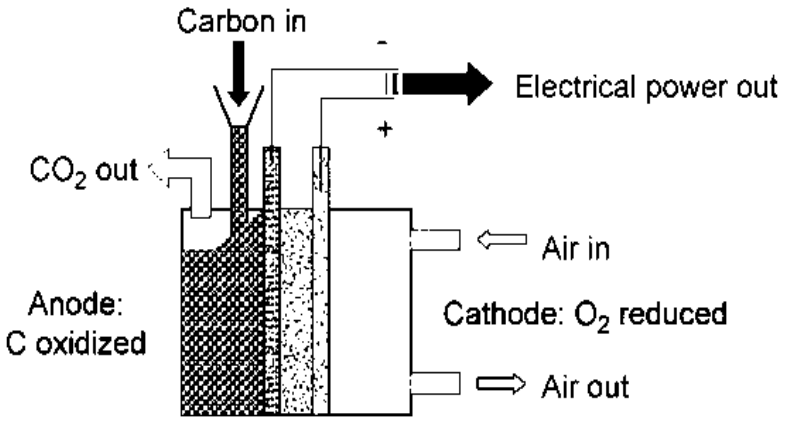

Figure 2.1: Schematic of a direct carbon fuel cell configuration (Cao et al., 2007)

2.3 DCFC configurations

Producing electricity from carbonaceous material without any pretreatment was one of the biggest dreams of electrochemists. The first attempt to do so, was made by William Jacques in 1896 when he built the first large scale fuel cell (Jacques, 1896). Driven by curiosity, scientists have been studying the different possible configurations of DCFC and trying to identify the key factors that will improve efficiency to start the production of fuel cells on industrial scale. Fuel cells have very similar basic structures; they consist of a cathode in contact with an electrolyte which is an ion conductor, and the circuit is completed with the anode in contact with the electrolyte. The major characteristic of a DCFC is that the fuel used is a solid carbonaceous material which will react directly at the electrode to form a gaseous product (CO_2). For other types of fuel cells, the fuel used is either gaseous (exp: hydrogen fuel cell, methane fuel cell) or liquid (exp: methanol fuel cell).

DCFCs can be divided to three main families based on the electrolyte used (molten hydroxide, molten carbonate or oxygen ion conducting ceramic electrolyte) as described in Table 2.1. These families can contain different categories of DCFC based on the design of the anode chamber (Anode is the fuel itself, molten metal anode…). In this section, the different families of DCFC with high operating temperature (>500° C), which are under development will be reviewed in detail. Their technologies and challenges will also be highlighted.

Table 2.1: Main types of direct carbon fuel cells and fuel cell reactions (Giddey et al., 2012).

Fuel / Anode	Electrolyte	Cathode	T, °C
Solid graphite rod as fuel & anode $C + 4OH^- = 2H_2O + CO_2 + 4e^-$	Molten Hydroxides OH^- ←	Air as oxidant $O_2 + 2H_2O + 4e^- = 4OH^-$	500 - 600
Carbon particles as fuel in MC & anode $C + 2CO_3^{2-} = 3CO_2 + 4e^-$	Molten Carbonates CO_3^{2-} ←	Air as oxidant $O_2 + 2CO_2 + 4e^- = 2CO_3^{2-}$	800
Concept1: Carbon particles in a fluidised bed $C + 2O^{2-} = CO_2 + 4e^-$	Oxygen ion conducting ceramic electrolyte O^{2-} ←	Air as oxidant $O_2 + 4e^- = 2O^{2-}$	700 – 900
Concept2: Molten tin + C $Sn + 2O^{2-} = SnO_2 + 4e^-$ $SnO_2 + C = Sn + CO_2$		Air as oxidant $O_2 + 4e^- = 2O^{2-}$	
Concept3: Molten salt + C particles $C + 2O^{2-} = CO_2 + 4e^-$		Air as oxidant $O_2 + 4e^- = 2O^{2-}$	

2.3.1 DCFC with molten hydroxide

William Jacques was the first person to build a large scale direct carbon fuel cell of this type in 1896 (Jacques, 1896) (Figure 2.2-a, 2.2-b). Generally this type of DCFC is made of a metallic container which is not only acting as the cathode but also will contain the molten hydroxide (commonly NaOH or KOH). The anode is a rod made of the solid fuel (carbon-rich material) and is dipped in the molten electrolyte.

In this family of fuel cells, the mobile charge species is the hydroxide ion and the cell reactions are shown in Equations 2.2-2.4.

Anode: $C + 4OH^- = 2H_2O + CO_2 + 4e^-$ (2.2)

Cathode: $O_2 + 2H_2O + 4e^- = 4OH^-$ (2.3)

Overall reaction: $C + O_2 = CO_2$ (2.4)

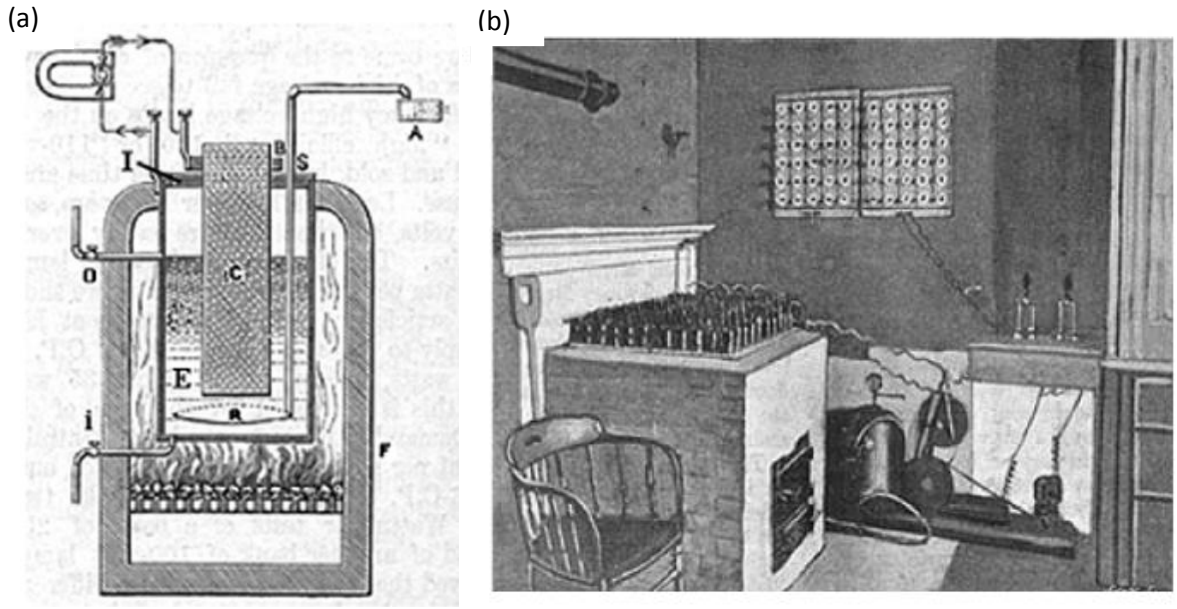

Figure 2.2: (a) A schematic of a DCFC built by William Jacques in 1896. (b) Apparatus used by William Jacques. A: air pump, B:anode current collector, C:carbon anode, E: coustic soda solution , F: fuel cell furnace, I: iron receiver connected to the cathode (reservoir), i: iron tube to discharge the solution, o: iron tube for the admission of the solution, R: air performed nozzle, S: insulator collar to hold the carbon anode (Jacques, 1896)

William Jacques cells produced a current density of 100mA/cm2 at 1 V (Jacques, 1896) after putting 100 of them in series. However, this design had several problems such as:

- chemical contamination due to impurities in the carbon material used,
- the formation of carbonates within the electrolyte which caused high degradation rates.
- Negligence of the thermal energy of the furnace and the power consumed by the air pump, thus energy efficiency was only 8%) (Jacques, 1896)

One of the biggest issues for such a design is the carbonate formation due to the reaction of hydroxide ions with CO_2. This phenomenon was explained by Goret and Tremillo (1967), and they found out that the carbon was easily oxidized at the carbon anode to give carbonate ions according to the reaction in Equation 2.5. Also the CO_2 produced at the anode reacted with the hydroxide ions to generate carbonates as shown in Equations 2.5 and 2.6.

$$C + 6OH^- - 4e^- \rightarrow CO_3^{2-} + 3H_2O \qquad (2.5)$$

$$2OH^- + CO_2 \rightarrow CO_3^{2-} + H_2O \qquad (2.6)$$

The formation of carbonate ions caused quick degradation of the molten hydroxide electrolyte since they are not electro-actif which will make the system very slow.

In order to inhibit the formation of carbonates, Goret and Tremillo (1967) investigated the mechanism behind the formation of these ions. They found that the production of carbonate ions (Equation 2.5) is achieved in two steps (Equations 2.7-2.8).

A fast chemical step: $6OH^- = 3O^{2-} + 3H_2O$ (2.7)

A slow electrochemical step: $C + 3O^{2-} \rightarrow CO_3^{2-} + 4e^-$ (2.8)

They concluded that the water present is extremely important to inhibit the carbonate formation because it indirectly slows down the O^{2-} generation in favor of hydroxide ions formation which is the mobile entity that kept the DCFC system running. The addition of water also increased the ionic conductivity of the molten electrolyte and helped to reduce the corrosion rate of nickel, iron and chromium that are present in the other cell components (Zecevic et al., 2004).

In the mid 1990s, Scientific Applications and Research Associates Inc. (SARA) (Cypress, CA) focused on DCFC based on molten hydroxide, they saw a lot of advantages in this type of DCFC. First, the electrolyte will insure a high ionic conductivity, and better reactivity with carbon (Herold et al., 1996) which will lead to a higher electrochemical reactivity at the anode which in turn leads to higher anodic oxidation rates and lower over potential losses (Zecevic et al., 2005). The hydroxides used for the fuel cell, had relatively low melting point (318.4° C) which implied, moderate operating temperature for the fuel cell (400 to 600° C) which can be built from less expensive materials (Pesavento, 1999). The lower operating temperature also favors the oxidation of carbon to CO2 rather than CO (the reverse Boudouar reaction is favored above 700° C). All of the previously mentioned advantages were believed to increase the fuel utilization and thus the overall system efficiency.

Trying to solve the design and undesirable reaction problems, SARA continued to develop its technology. Figure 2.3-a shows a schematic view of the hydroxide based direct carbon fuel cell design used by SARA in most of their investigations. Their DCFC used a simple design in which graphite rods served as the fuel and anode, while the metal alloy containers served as the cathode. The cell was operated at 500-650 °C, and the cell performance was found highly depended on the cathode materials, air flow rate and the operating temperatures

(Zecevic et al., 2004). However, such a design had three main drawbacks (1) the air bubbled in the electrolyte, comes in contact with the anode, resulting in the chemical consumption (rather than electrochemical) of solid carbon to generate carbon dioxide, (2) the carbon anode needs to have a specific geometry, which makes it difficult to continuously fuel the cell, (3) the exhaust gas was a mixture of depleted air and the CO_2 which needed a more sophisticated CO_2 capture technology. (Patton and Zecevic, 2005).

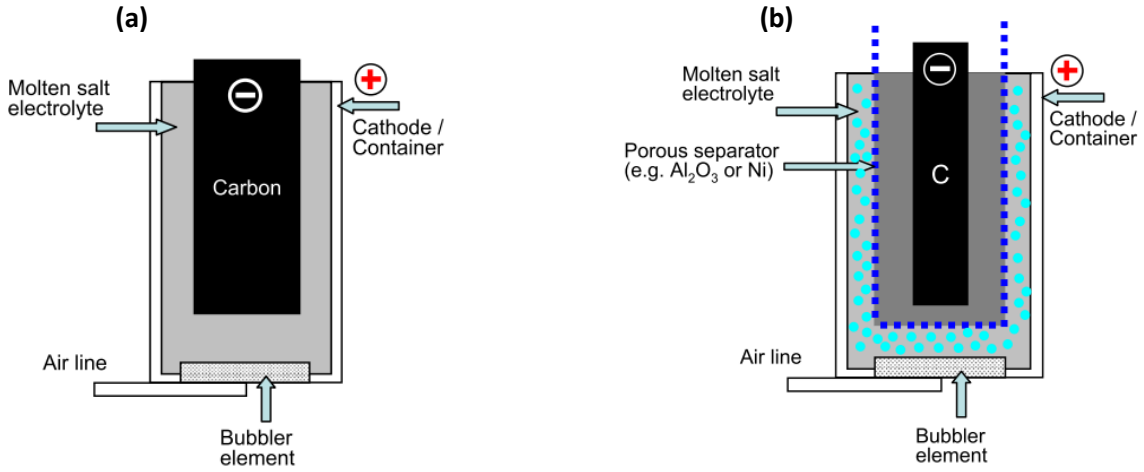

Figure 2.3: A schematic drawing of (a) the original DCFC and (b) the modified one, used by SARA in most of their investigations. (Zecevic et al., 2004; Patton and Zeicevic 2005)

In order to overcome the previously mentioned drawbacks, a new design (Figure 2.3-b) was proposed by Patton and Zecevic (2005) and consisted on the addition of a porous separator which will prevent two phenomena from occurring (1) the oxygen from coming in direct contact with the carbon anode and (2) the mixing of CO_2 and the air dissolved in the electrolyte. Such a design improved the cell efficiency, made it possible to use a variety of fuels, and made the system more compatible with the CO_2 capture technology. The latest prototypes used by SARA are MARK II-D and MARK III-A and their performance is shown in Figure 2.4:

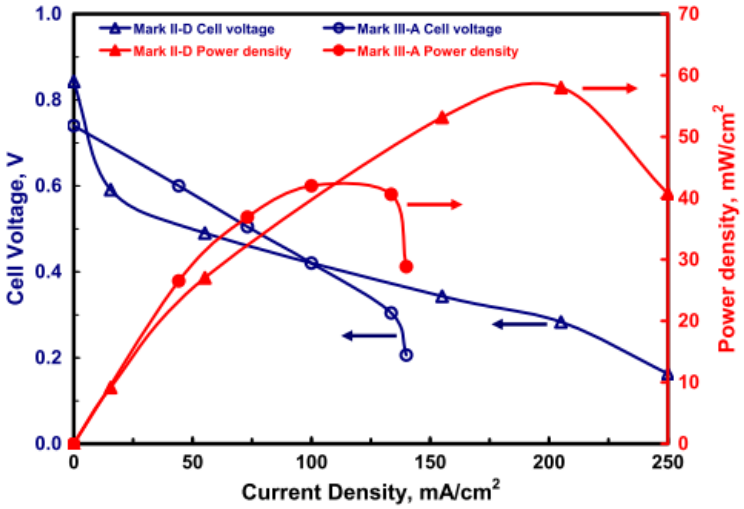

Figure 2.4: Voltage-current density and Power density-current density curves of MARK II-D and MARK III-A at 630° C. (Patton and Zecevic, 2005).

Fig. 4 shows the voltage and power density versus current density characteristics of SARA's MARK II-D and MARK III-A DCFCs at 630° C.

The voltage-current density characteristics show that a maximum power density of 58mW/cm2 was obtained at 200mA/cm2 and a limiting current condition was reached beyond 250mA/cm2. The open circuit voltage varied between 0.75 and 0.85 V. A lifetime of 540 hours was produced by the Fe_2Ti cathode. The maximum efficiency measured in the MARK III-A prototype was 60% at 50 mA/cm2.

The latest design developed by SARA for a molten hydroxide based fuel cell, which is planned to be a commercial prototype, is shown in Figure 2.5. In this design, the carbon particles (anode-fuel) are located in a screen type anode current collector. A porous separator is surrounding the anode compartment to prevent the direct contact of air with the carbon particles and to prevent the mixing of CO_2 and air. The cathode compartment is a metallic rectangular container which surrounds the separator. The space between the separator and cathode wall contain the molten hydroxide. A pump supply air to the hydroxide melt.

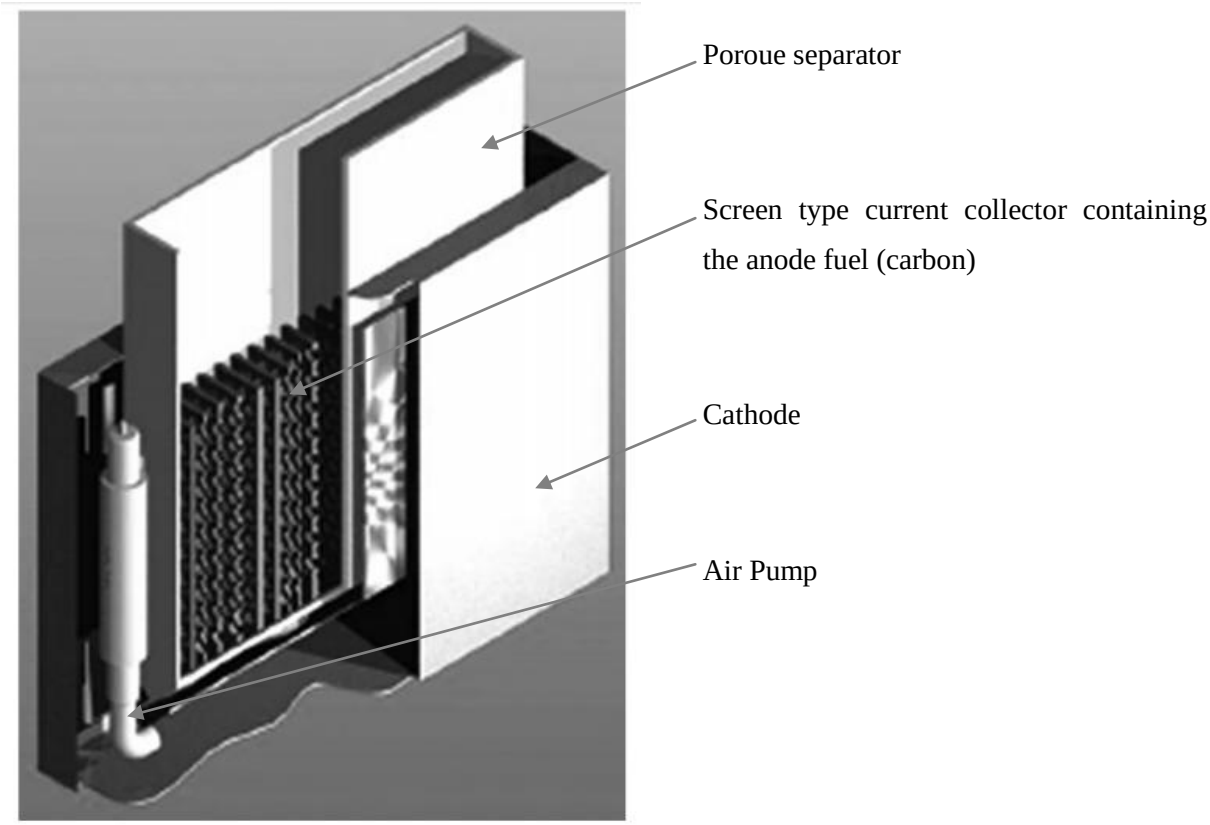

Figure 2.5: Concept sketch of the commercial DCFC proposed by SARA (Patton and Zecevic, 2005).

Despite all the advantages mentioned above, corrosion is a common problem present in any system working at high temperature and in the presence of electroactif ions, including fuel cells. The degradation level of the molten hydroxide electrolyte is proportional to the corrosion rate and temperature. In order to reduce the operating temperature, an eutectic of sodium hydroxide and lithium hydroxide was used, allowing the system to work at a relatively low temperature which reduced the corrosion rates of metals used in the fuel cell.

2.3.2 DCFC with molten carbonate

Broers and Ketelaar (1960) reported a high temperature fuel cell in which, hydrogen is the fuel and carbonate ions (CO_3^{2-}) were the means of charge transport within the molten electrolyte comprising a mixture of alkali metal carbonates constrained within a disc of magnesium oxide.

The reaction equations for this system are presented in Equations 2.9-2.11 (Dicks, 2004).

$$\text{Anode: } 2H_2 + 2CO_3^{2-} \rightarrow 2H_2O + 2CO_2 + 4e^- \qquad (2.9)$$

$$\text{Cathode: } O_2 + 2CO_2 + 4e^- \rightarrow 2CO_3^{2-} \qquad (2.10)$$

$$\text{Overall: } 2H_2 + O_2 \rightarrow 2H_2O \qquad (2.11)$$

One of the characteristic of such fuel cell is that the CO_2 is directly transferred from the cathode compartment to the anode compartment as shown in Figure 2.6.

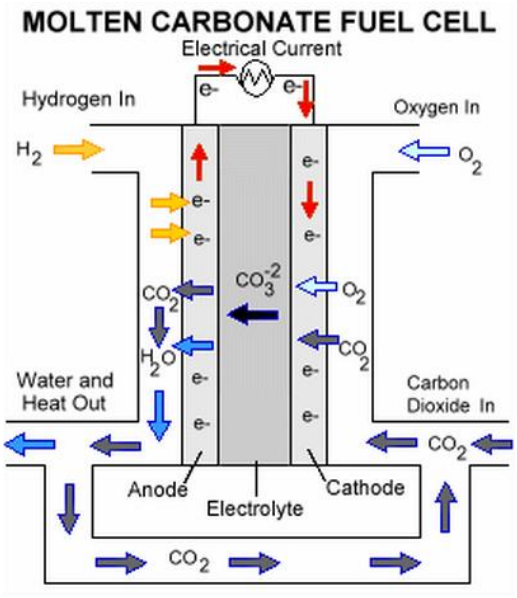

Figure 2.6: Working Principle of a Molten Carbonate Fuel Cell Fuel Cell (Verhaert net al., 2009)

Since then, researchers have been trying to develop new designs and technologies in order to build an optimized fuel cell.

Solid carbon is another abundant material that can be used as a fuel for Molten Carbonate Fuel Cell (MCFC). Compared to hydrogen, carbon is much easier to handle and safer than hydrogen. Also a system which is working with hydrogen is much more expensive than the one working with solid carbon. The reactions occurring within a carbon fuel based MCFC are represented in Equations 2.12-2.14. (Cooper, 2007).

$$\text{Anode} \quad C + 2CO_3^{2-} = 3CO_2 + 4e^- \tag{2.12}$$

$$\text{Cathode} \quad O_2 + 2CO_2 + 4e^- = 2CO_3^{2-} \tag{2.13}$$

$$\text{Overall reaction} \quad C + O_2 = CO_2 \tag{2.14}$$

So far, it has been shown that it is possible to operate a molten carbonate fuel cell system on solid carbon fuels with electric efficiency as high as 80% with near 100% fuel utilization. (Cooper, 2007; Dicks, 2004; Vutetakis and Skidmore, 1987; Giddey et al., 2012).

A lot of design have been adopted and tested. In 1987, Vutetakis and Skidmore (1987) developed a DCFC which used coal as fuel dispersed in slurry of molten carbonate (Figure 2.7). The working electrode was a solid gold rod cemented to the end of an alumina tube using zircar alumina cement to cement and seals the gold rod to the alumina tube. The reference electrode was an alumina tube filled with oxygen, carbon dioxide, carbonate and gold. The counter electrode was an alumina tube containing a graphite rod. These electrodes in addition to the gas inlet/outlet tubes were sealed with a brass lid. They reported a high current density (108 mA/cm² at -0.3V and 700° C) that is due, according to them, to fast kinetics and mass transfer rates which resulted from stirring of the slurry with carbon particle in it. Furthermore, the stirred coal slurry overcame the anode shedding problem which had arisen with coal-derived anodes.

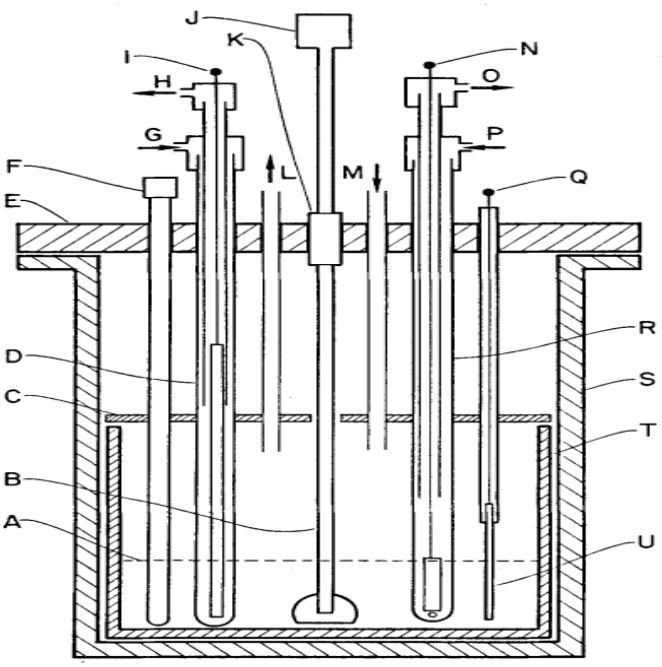

Figure 2.7: Fuel cell set up used by Vutetakis et al, To test different types of carbonaceous materials in a molten carbonate electrolyte. A: electrolyte level; B: shaft for stirring; C: crucible lid; D: counter electrode assembly; E: lid; F: thermocouple; J: motor for the stirring shaft L: outlet for the cell purge; M: inlet for cell purge; R: Reference Electrode assembly; inconel canister; T: crucible made of alumina; U: gold Working Electrode. (Vutetakis and Skidmore, 1987)

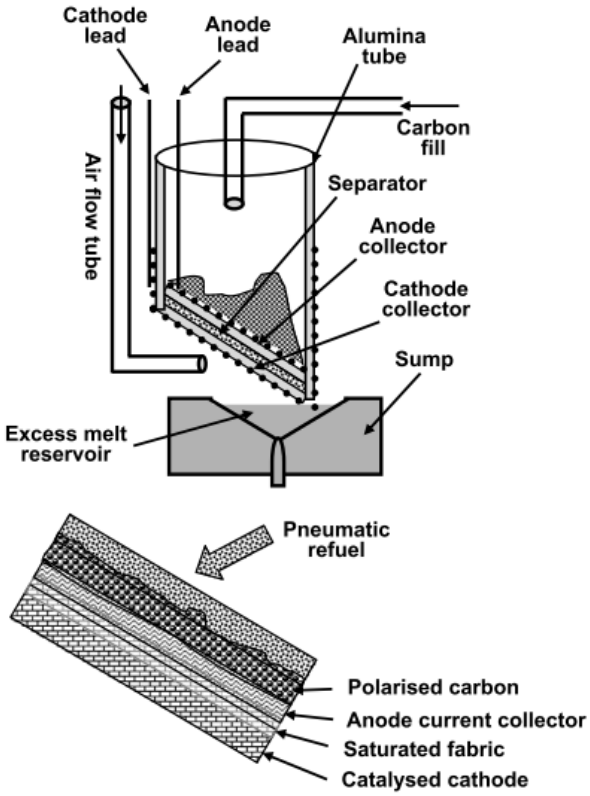

Figure 2.8: A schematic representing the tilted Direct Carbon Fuel Cell configuration adopted by LLNL (Cooper, 2003).

Cooper et al. (2007) designed a MCFC which is shown in Figure 2.8. In this design, there is no geometric limitation of the carbon fuel. Carbon is supplied to the system mixed with the molten carbonate electrolyte. The anode was made of a mixture of carbon particles and carbonate electrolyte in contact with an inert metal current collector (Nickel foam). The cathode was made of nickel oxidized in the presence of lithium. A zirconia based porous separator was placed between the anode and cathode and it ensured the transfer of carbonate ions between the two electrode compartments. Since the molten carbonate was in excess in this system, flooding of the cathode could occur while the fuel was consumed. As a solution for this problem, the container bottom had an angle of 5-45° to the horizontal to allow the excess of molten electrolyte to be drained.

The performance of the fuel cell designed by Cooper et al. (2003) at the Lawrence Livermore National Laboratory (LLNL) is shown in Figure 2.9.

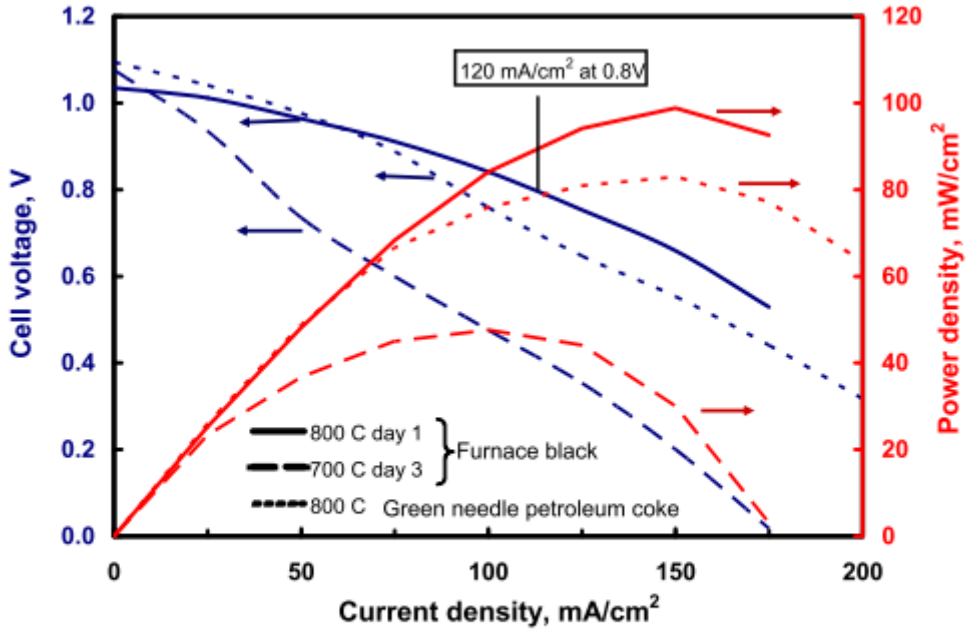

Figure 2.9: Voltage- current density curves and Power density - current density curves obtained after using carbon black as the fuel. The fuel cell shows a current density superior to 100mA/cm² (Cooper, 2003).

A maximum current density of 120 mA/cm² at 0.8V was recorded at 700° C (power density of 40 mW/cm²) for the carbon black and when the temperature was increased to 800° C, the current density was 160 mA/cm² at 0.63V and a power density of 96 mW/cm² was recorded. (Cooper, 2003).

Predtechenskii et al. (2010) conducted a lot of experiments in which they optimized a design for the MCFC. Figure 2.10 represents the design they proposed, and it shows simplicity and has high specific characteristics (current density and specific power values). (greatest achieved power per unit surface of the anode unit was 120 mW/cm2 at 155 mA/cm2 when the fuel was polyethylene terephthalate (PET) plastic.

This fuel cell could use different types of carbon and even organic fuels, and it was shown that the fuel oxidation rate and the maximum achievable specific power were proportional to the amount of hydrogen in the organic fuel.

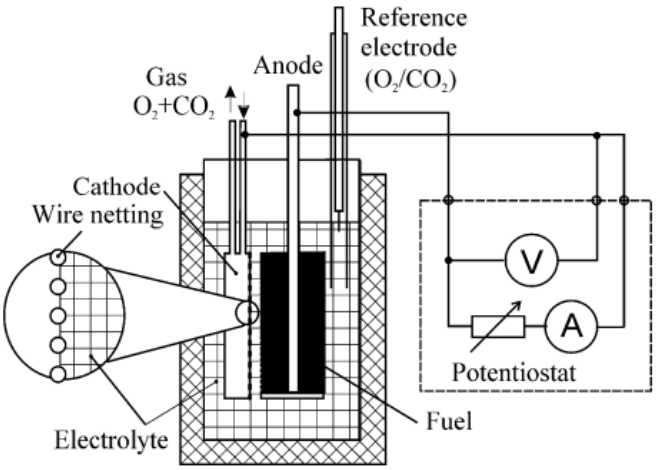

Figure 2.10: A schematic of the molten carbonate electrolyte fuel cell proposed by Predtechenchkii (Predtechensky et al., 2009).

The corrosion problem was present in this type of fuel cell since the two main corrosion parameters; high temperature and carbonate ions. Because carbonates generally have higher melting point than hydroxides, the corrosion rates in the MCFC were higher than in MHFC. However, the MCFC had several advantages such as high conversion efficiency, the production of a very concentrated stream of pure CO2 in the product gas (which made CO_2 separation unit unnecessary) (Wolk, 2004), the high ionic conductivity (Glugla and DeCarlo, 1982), the long term stability of molten carbonates in the presence of CO_2 (Tanimoto et al., 1998), and the catalysis of carbon oxidation reaction (McKee and Chatterji, 1975).

In another work Li et al. (2010) showed that the pressure of CO_2 influenced the cell voltage described in Equation 2.15.

$$E_{cell} = E^{\circ} - \left(\frac{RT}{4F}\right) \ln[P^3_{CO_2}(w)] + \left(\frac{RT}{4F}\right) \ln[P^2_{CO_2}(r)\, P_{O_2}(r)] \qquad (2.15)$$

Where: E°: the anode potential at standard condition, R: universal gas constant, T: cell temperature (K), $P_{CO2}(w)$: CO_2–partial pressure to total pressure at the working electrode, $P_{CO2}(r)$ and $P_{O2}(r)$ are the partial pressures of CO_2 and O_2 to total pressure at the reference electrode, respectively.

Like other types of DCFCs, the mechanism of carbon reactions in the molten carbonate based DCFCs is not yet fully understood. A lot of mechanisms have been suggested by different groups of researchers in order to solve the carbon reactions mechanisms.

Cherepy et al. (2005) proposed a set of equations (Equation 2.16-2.22) explaining a possible electrochemical mechanism behind CO_2 production at the anode area.

$$2CO_3^{2-} = 2CO_2 + 2O^{2-} \quad \text{Carbonate dissociation} \tag{2.16}$$

$$C_{RS} + O^{2-} = C_{RS}O^{2-} \quad \text{Fast adsorption on carbon reactive sites} \tag{2.17}$$

$$C_{RS}O^{2-} = C_{RS}O^{-} + e^{-} \quad \text{Fast discharge} \tag{2.18}$$

$$C_{RS}O^{-} = C_{RS}O + e^{-} \quad \text{Fast discharge} \tag{2.19}$$

$$C_{RS}O + O^{2-} = C_{RS}O_2^{2-} \quad \text{Slow adsorption : Rate determining step} \tag{2.20}$$

$$C_{RS}O_2^{2-} = C_{RS}O_2^{-} + e^{-} \quad \text{Fast discharge} \tag{2.21}$$

$$C_{RS}O_2^{-} = CO_2(g) + e^{-} \quad \text{Fast discharge and gas evolution.} \tag{2.22}$$

Where:

C_{RS}: reactive site on the carbon fuel surface.

O^{2-}: product of the dissociation of carbonate ions at high temperature.

The key factor on which this mechanism of CO2 production is based on the oxygen adsorption on the anode surface which is in direct relation with the surface area of the anode, the frequency of the reactive sites (C_{RS}) and the wetting ability of the fuel (Cherepy et al., 2005). A comparative study of different carbon sources was made by Li et al. (2010) and they found that the reaction rates of carbon in the molten carbonate electrolyte are in direct proportion to the surface area, the chemical composition, the nature of the mineral matter in their ashes, and the number of oxygen surface groups of the carbon-rich material used. They also found out that the presence of minerals such as Al_2O_3 and SiO_2 had inhibitive effect on the anodic reaction, while CaO, MgO and Fe_2O_3 had catalytic effect on the electrochemical oxidation of carbon.

Lee et al. (2011) tested activated carbon made from bamboo on a coin-type MCFC, represented in Figure 11, in which the carbon fuel was supplied through an aluminum tube at the anode which ensured the availability of carbon for reaction. They found that carbon was first oxidized to CO via chemical route (Equation 2.23), and then CO_2 was obtained after electrochemical oxidation of CO (Equation 2.24).

$$C + CO_3^{2-} \rightarrow 2CO + O^{2-} \quad (2.23)$$

$$CO + CO_3^{2-} \rightarrow 2CO_2 + 2e^- \quad (2.24)$$

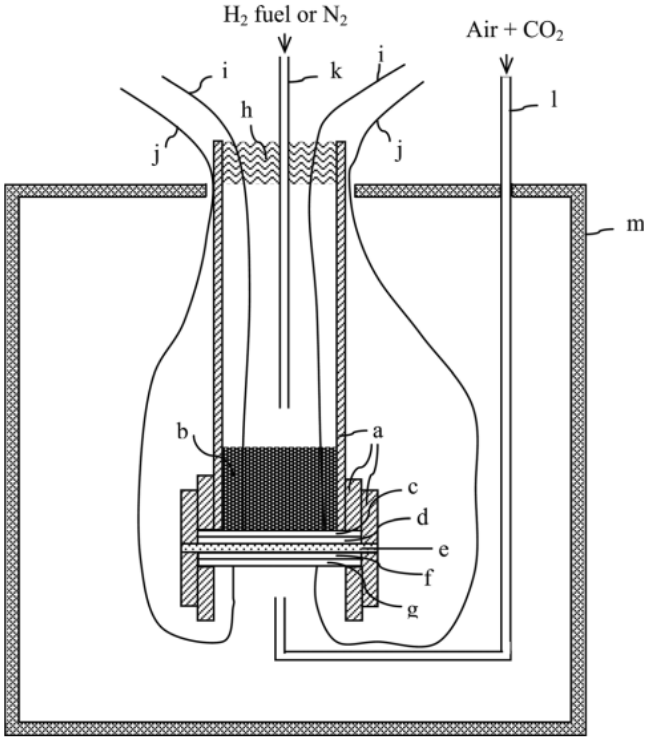

Figure 2.11: Drawing representing a coin type direct carbon fuel cell system (a) tube made of alumina, (b) carbonate and carbon slurry, (c) current collector of the anode, (d) anode, (e) matrix, (f) cathode, (g)current collector of the cathode, (h) thermal isulator (glass wool), (i) anode lead, (j) cathode lead, (k) gas inlet, (l)cathode gas inlet, and (m)furnace heated with electricity. (Lee, et al., 2011)

2.3.3 DCFC with solid oxide oxygen ion conducting electrolyte technology

The discovery of solid oxide electrolyte in 1899 by Nernst led to the emergence of solid oxide fuel cell (SOFC). It was reported that unlike pure metal oxides which have low conductivity at high temperature, mixtures of metal oxides can have much higher conductivity under similar temperature and pressure conditions, these studies resulted in the 'Nernst glower' which was the first practical use of solid oxide.

The first patent of a solid oxide fuel cell (Figure 2.12) was patented by Haber (1907) who used platinum and gold as the electrode materials and glass (from 330 to 570° C) and porcelain (from 800 to 1100° C) as the electrolyte.

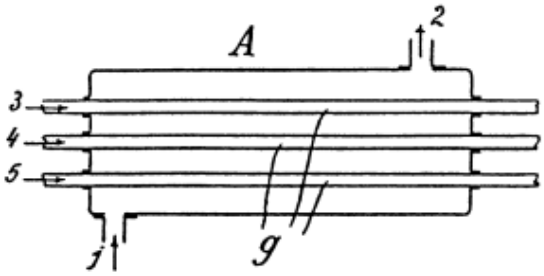

Figure 2.12: Nernst's fuel cell with solid electrolytes. Generator gas passed from 1 to 2 through chamber A (440°C) g: parallel glass tubes covered on both sides with thin layers of noble metal and swept inside by air.(Haber, 1907).

2.4 Benefits of DCFC

Unlike other types of fuel cells whose fuel utilization within the cell is usually below 85%, the DCFC can reach a fuel utilization efficiency that can go up to 100% since it has the potential to convert the chemical energy of carbon directly into electricity without the need for gasification or the moving machinery associated with conventional electric generators, thus the product gases and fuel feed are completely separated. Moreover, the theoretical efficiency of DCFC is also high (close to 100%). All of the previously mentioned factors lead to the conclusion that DCFC can have a thermodynamic efficiency up to 80%, which is approximately twice the efficiency of current generation of coal fired power plants. This implies a 50% reduction of greenhouse gas emission, especially carbon dioxide (CO_2) which is the major cause of the global warming. In addition to all of these advantages, the solid

carbon fuels are abundant and easy to collect and organic wastes (organic garbage, agricultural residues, industrial used oils…) can be a potential resource of carbon rich materials. (Hackett et al., 2007; Giddey et al., 2012; Cao et al., 2007).

2.5 Challenges with the DCFC

As a high temperature operating fuel cell, the different types of DCFC have to face numerous challenges in order to optimize a fuel efficiency that meets the industrial requirement for scale-up and prolonged lifetime.

Giddey et al. (2012) mentioned in their review that the technical issues faced with MCFCs are cathode polarisation, loss of cathode performance with time, corrosion of metal bipolar plates, difficulties associated with fuel delivery, low power densities, short cell lifetimes and the need to keep the cell under constant polarisation to avoid the reverse Boudouard reaction. Moreover, the need for a suitable fuel delivery system and the relationship between the carbon structure and its electrochemical activity is still to be fully established.

The most critical challenges faced by DCFCs researchers are: high temperature related corrosion, carbon fuel reaction mechanism, fuel physical and chemical requirements, and the lifetime of the fuel cell.

2.5.1 High temperature related corrosion

One of the major challenges facing DCFCs is the effect of high temperature on the cell's components. This problem is less significant for MCFC compared to SOFCs since Weaver et al. (1981) reported that at a carbonate temperature of 700° C the carbon was completely oxidized. This finding made a big difference on the lifetime of fuel cell components and system performance. Since then, a lot of interest has been given to MCFCs. Weaver et al. (1979) developed a ternary eutectic of Lithium/Sodium/Potassium carbonates, and found that in addition to the low operating temperature, this carbonate slurry had a scavenging capability for the pollutants produced by coal such as ash and sulfur compounds, which can cause dramatic drop in cell performance.

Despite these reports, DCFC performance is proportional to the temperature, so expensive materials are needed to operate the fuel cells at high temperatures. One of the goals of researchers has been to lower the cell operating temperature, while keeping its performance

as high as possible. Kouchachvili and Ikura (2011) developed an electrolyte mixture consisting of 43.5 mol % Li_2CO_3, 31.5 mol% Na_2CO_3, 25 mol % K_2CO_3 and they added 20 wt% Cs_2CO_3). They reported that this complex electrolyte could function effectively at temperatures as low as 650° C-700° C and achieve comparatively high DCFC performance.

2.5.2 Carbon fuel reaction mechanisms

Understanding the fundamental mechanisms of carbon oxidation and their dependency on various cell designs and operating parameters is crucial for the optimisation of the DCFC efficiency. Unfortunately, the lack of instrumentation that can detect reaction intermediate products and ions at high temperature are not available. However, an indirect method, which consisted on the analysis of the off-gas, was used to study the electrochemical oxidation of carbon in DCFC. Weaver et al. (1981) reported that the anode off-gas was 90% CO_2. Vutetakis et al. (1985) reported that the anode off-gas was manly CO_2 at 600-800° C, however, the CO% increased with the decreased current density. Moreover, Cao et al., (2007) reported that both CO_2 and CO exist at the anode off-gas. Therefore, the origin of CO needs more investigations to conclude whether it is generated by the chemical reaction of carbon and CO_2 via Boudouard reaction ($C+CO_2 \rightarrow CO$), or it was the electrochemical oxidation of carbon.

The oxidation of carbon in molten carbonate electrolytes was studied by Cherepy et al., (2005). They suggested the mechanism detailed in Equations 2.16-2.22 (Section 2.3.2).

Hasegawa and Ihara (2008) explained the carbon oxidation mechanism in the case of a solid oxide fuel cell where a three phase (solid carbon/anode/solid oxide electrolyte) boundary is needed. In this case, the cell performance was related to the number of available reaction sites at the boundary.

2.5.3 Fuel physical and chemical requirements for DCFC

The physical and chemical properties of the carbon fuel have an important role on the DCFC performance. Carbons with disordered structure and high surface area, which offer larger interaction interface between the carbon particles and the ions in the electrolyte. This interaction interface can be increased by reducing the particle side of the carbon fuel.

Li et al. (2010) reported that an acid treatment of the coal enhanced its electrochemical reactivity and they explained this improvement by the increase in oxygen-containing surface functional groups, particularly CO_2 -yielding surface groups. By contrast, the elimination of

these groups by heat treatment resulted in a sharp decrease in the electrochemical reactivity in the DCFC. Also, the removal of impurities such as ash and organics from the carbon-rich fuel would yield an increase in the performance of the fuel cell. Moreover, the effect of higher surface area of carbon can be beneficial to the fuel cell performance, but much less important than surface chemistry (Kim et al., 2001).

2.5.4 Lifetime of the fuel cell

The life time of the fuel cell is directly related to the lifetime of its components (electrolyte, anode and cathode). Zecevic et al. (2005) reported that the cathode material and surface area can improve the performance of the fuel cell and prolong its lifetime. On the other hand, Cooper et al. (2005) knew how to prolong the life time of their fuel cell, and they did this by changing the geometry of the system in a way to avoid the flooding of the cathode by the electrolyte as the fuel was consumed, and this prolonged the fuel cell life to 12 hours.

Gür et al. (2010) studied the effect of sulphur on anode performance. They reported a decrease in fuel cell performance and degradation of components with increasing amount of H_2S injected to the system.

More investigations on the effect of Sulphur, ash and other minerals contained on the carbon fuels is needed in order to identify the appropriate anode materials and the appropriate fuel feed systems.

2.6 Carbon as a fuel

2.6.1 Overview of carbon:

Carbon has been known as a unique element that forms more compounds than all other elements combined. Carbon is widely distributed as elemental and compound forms, it accounts for about 0.03% of the atmosphere in the form of CO_2, and it is one of the basic elements that constitute the earth's crust.

In today's world, one of the most important sources of energy for the industry is amorphous forms of carbon such as coal, which can be also used as raw material for manufactured carbon and graphite. The applications of carbon are numerous and vary from rocket nozzles- where heat tolerance is required- to the ubiquitous "lead" in pencils. (Banks, 1990).

Many forms of carbon exist between the two extreme structures of graphite and diamond. The common ones that have been of interest for fuel cells are: coal, graphite, activated carbon, carbon black and carbon nanofibers.

Li et al. (2008) reported that a desirable carbon fuel for DCFC should have high mesoporous surface area (to ensure a high efficiency of electrolyte transfer) and rich oxygen-containing surface groups (to provide a higher degree of reactive sites on the surface of the carbon fuel). The anodic performance of the DCFC may also be improved by small carbon particle size.

2.6.2 Physical and chemical properties of the different carbons

2.6.2.1 Graphite

Graphite is known to be a good electricity conductor due to its highly organized and compact structure. The good electrical conduction property of graphite is due to the π electrons, which are the valence electrons that are not involved in the sp^2 hybrid bonds holding every layer of carbon atoms together. These free π electrons explain also the reactivity of graphite with its environment without disturbing the layer structure. Moreover, the electrical conductivity of graphite can vary depending on the availability of the π electrons, which can be involved in the reaction with an atom, molecule or ion that got intercalated between the structure layers. (Dicks, 2006). However, due to the highly organized structure, the external surface of graphitic carbon has only few lattice defect and active edge carbon. This can be a disadvantage when surface active sites are needed for the anodic half reaction in the case of a DCFC. In addition to that, and in case of a molten electrolyte, graphite has a poor wetting ability due to its compact structure, but also due to the presence of hydrophilic surface functional groups, which lower the performance of the fuel cell. These drawbacks of a graphite anode leave us with the conclusion that graphite alone cannot perform well as anode material in DCFC although it has regular structure, high electrical conductivity and low resistance (Chen et al., 2010).

2.6.2.2 Carbon black

Carbon black is obtained by the decomposition of liquid or gaseous hydrocarbons at elevated temperature under a reduced presence of oxygen (Donnet et al., 1993). The most known carbon black nowadays is “furnace black” which is obtained by immediate water quenching of partially combusted hydrocarbons.

For application on DCFC, there are two types of carbon black that can be used as a potential fuel; acetylene black and PUREBLACK® carbon. Acetylene black, which is obtained by partial oxidation of acetylene gas, has a high aggregate structure and crystal orientation, these two characteristics make acetylene black very valuable as an electrical conductor and as an electrolyte absorber in battery systems. On the other hand, PUREBLACK® Carbon has a graphitic structure that is synthesized from furnace black in a fluidized bed (Wissler, 2006). The purpose of the graphitization treatment is to increase the conductivity and purity of the material. In addition to that, and due to the organized structure of graphite, the surface of PUREBLACK® has less reactive sites, thus becomes less reactive with its environment i.e. the humidity absorption and solvent adsorption decrease dramatically after the graphitization treatment. These features make the product an easy-to-handle conductive additive for lithium-ion batteries and other electrochemical systems (Wissler, 2006).

The manufacturing process has a high influence on the morphology and the physicochemical properties of carbon black.

2.6.2.3 Activated carbon/charcoal

"Activated carbon" is a vaguely used term referring to a family of carbon-based adsorbents with extremely developed internal pore structure and highly crystalline forms. The term activated carbon is more frequently used to design activated coal while activated carbon obtained from woody precursors is called "activated charcoal". Charcoal is obtained by carbonization of wood in a limited supply of oxygen. Pyrolysis is one of the modern ways to obtain charcoal (Antal and Gronli, 2003).

During carbonization, chemical bonds are fractured and the biomass structure is rearranged to form aromatic structures. Since these transformations don't occur in liquid phase, many bonds are left dangling leading to a carbonaceous product which is porous, has a large surface area, and highly reactive (Antal and Gronli, 2003).

One of the results of the high reactivity of charcoal is the chemisorptions of water and oxygen from its environment, leading to the formation of oxides and peroxides on its surface (Wenzl, 1970). Increased oxygen content decreases greatly the electrical conductivity of charcoal (Golden et al., 1983).

Charcoal conduct electricity as good as graphite, thus charcoal can be used as electrode (Coutinho et al., 2000). The electrical conductivity of charcoal is proportional to temperature

increase and it can attain values above 1 S/cm at temperatures above 900° C (Wenzl, 1970). The electrical conductivity of charcoal is negatively affected by the oxygen-containing functional groups. However, these functional groups would provide higher degree of reactive sites for the electrochemical oxidation of carbon particles within the charcoal (Li et al., 2008).

Porosity of charcoal is proportional to the carbonization temperature (Baileys and Blankenhorn, 1982; Wenzl, 1970). Pore volume range in the case of carbonized red wood was $1.8x10^{-7}$-$2.3x10^{-7}$ m^3/g (Mackay and Roberts, 1982).

If the temperature exceeds 1000° C, a strong falloff in the open micropore volume was observed (Baileys and Blankenhorn, 1982), leading to the generation of mesopores. Since mesopores provide more efficient electrolyte transfer than micropores, a carbonization temperature above 1000° C would yield a charcoal with a good wetting ability.

All the properties of charcoal are dependent on the peak temperature which is the maximum temperature at which the charcoal was carbonized.

Charcoal contains no sulfur or mercury. It is low in nitrogen and ash, compared to carbons from fossil fuel. These characteristics imply that charcoal is a purer form of carbon than graphite (Antal and Gronli, 2003), thus would give a better performance when used as a carbon fuel in DCFC, and would cause less corrosion to the DCFC at high temperature.

Depending on the raw material (example: coal, wood, lignite, coconut shell and peat as well as fruit pits, synthetic polymers or petroleum processing residues) (De la Torre, 2010) and the activation method used for their production, activated carbons/charcoals can acquire different characteristics and exhibit different behavior with their environment.

The final product of the physical activation process has a ‘fine’ pore structure, ideal for the adsorption of compounds from both the liquid and vapor phase. (Apelsa Guadalajara, Mexico; He et al., 2012; Nevskaia and Martin-Aranda, 2003).

Activated carbons/charcoals produced by chemical activation generally exhibit a very 'open' pore structure, ideal for the adsorption of large molecules (Apelsa Guadalajara, Mexico).

So the use of a chemically activated carbon as anode fuel for DCFC, would be more beneficial than using physically activated carbon, since the former would have very open

pore structure which means better wetting ability compared to the physically activated carbon.

The effect of acid and base treatment on activated carbons/charcoals has been studied in several occasions and it has been reported that the surface chemistry, porosity, surface area of activated carbons/charcoals can be modified by acid or base treatments while the physical properties remain unchanged. (Moreno-Castilla et al., 1998; Chen and Wu, 2003). Chen and Shunnian (2004) reported that the acid/base treatment of activated charcoal increases the oxygen-containing functional groups, which would generate more reactive sites on the activated carbon surface. Hence, the acid/base treatment of activated carbon/charcoal would make it a potential anode fuel for DCFC.

Moreover, pre-soaking the activated carbon in carbonate mixture (Li_2CO_3–K_2CO_3**)** increases considerably the electrochemical performance of the activated carbon (Cao et al., 2010). In fact, when activated carbon is pre-soaked in a carbonate mixture (carbonate mixture represents the electrolyte in the case of a MCFC), the electrolyte will have time to go through the activated carbon mesopores and the carbonate ions will have access to more carbon atoms, thus the electrochemical performance of the activated carbon will increase.

As a result of pre-soaking the activated carbon sample in a carbonate mixture, the onset potential negatively shifted by around 100 mV and the current density increased by around 50 mA/cm2. On the other hand, the non-oxidant acids (HF) treatments are more effective than oxidant acid (HNO_3) and base (NaOH) treatments. In addition to the influence of the surface containing oxygen functional groups, the enhancement in electro-oxidation performance is related to the increase in surface area and the expansion of pores structure due to the acid/base treatment as shown in Table 2.2. (Cao et al., 2010).

Table 2.2: Specific surface area and pore volume modification of activated carbon after acid and base treatments. (Cao et al., 2010)

Samples	Specific surface area/(m^2 g^{-1})	Total pore volume/(cm^3 g^{-1})	Micropore volume(<2 nm)/(cm^3 g^{-1})	Mesopore volume/(cm^3 g^{-1})
AC	958	0.535	0.338	0.197
AC-HF	1016	0.561	0.362	0.199
AC-HNO_3	976	0.548	0.350	0.198
AC-NaOH	965	0.543	0.346	0.197

2.6.2.4 Biochar

Biochar is the carbon-rich material produced, in a closed container, by so-called thermal decomposition, also called Pyrolysis, of organic materials (Biomass) under limited supply of oxygen (O_2), and at relatively low temperatures (< 700°C). (Lehmann and Joseph, 2009; Mohan et al., 2006). Pyrolysis temperatures above 500° C produces a biochar with the highest carbon content (80%) and the lowest carbon content (15 to 60%) was obtained at temperatures around 350° C (Streubel, 2011).

Depending on the feedstock, temperature and pyrolysis method, the characteristics of biochar are highly variable. Table 2.3, represents the strong dependence of ash content and organic carbon content of the biochar on the operating conditions (pyrolysis temperature and residence time).The process and method of production of the biochar, will decide for its application (Mohan et al., 2006; Behrendt et al., 2008).

Table 2.3: Production of biochar from poultry litter by pyrolysis at different temperatures. (Song and Guo, 2012).

Pyrolysis temperature (°C)	Reaction time min	Yield (%)[a]	Biochar ash (%)[b]	Biochar OC[c] (%)[b]	Feed OC retention (%)
300	372 ± 10	60.13 ± 0.26	47.87 ± 0.12	37.99 ± 0.50	64.32 ± 0.76
350	271 ± 8	56.17 ± 0.25	51.29 ± 0.40	37.65 ± 0.15	59.56 ± 0.40
400	225 ± 5	51.52 ± 0.07	56.62 ± 0.31	36.10 ± 0.54	52.38 ± 0.61
450	200 ± 7	48.69 ± 0.04	58.66 ± 0.46	35.22 ± 0.51	48.30 ± 0.55
500	175 ± 3	47.57 ± 0.13	60.58 ± 0.09	34.47 ± 0.49	46.18 ± 0.62
550	150 ± 8	46.62 ± 0.08	60.65 ± 0.07	33.88 ± 0.42	44.47 ± 0.50
600	130 ± 5	45.71 ± 0.14	60.78 ± 0.16	32.52 ± 0.33	41.85 ± 0.47

[a] % of dry feed mass.
[b] % of biochar mass.
[c] OC: organic carbon content.

Figure 2.13 a-e, shows the morphology of a switchgrass biochars obtained from different thermo-chemical processes (pyrolysis and gasification) (Brewer et al., 2009). It can be seen that the porosity and particle size were different from one biochar to the other, depending on the process used for the thermal decomposition. The increase in the biochar porosity, associated with a decrease of the particle size, was mostly due to the rapid heating of the biomass, which caused rapid devolatilization of the organic compounds. Consequently, reduced particle size and increased porosity were observed after the gasification and fast pyrolysis process. In general, gasification chars particles are bigger than the fast pyrolysis chars particles. (Boateng, 2007; Scala et al., 2006; Brewer et al., 2009). The fine particle size of the fast pyrolysis biochars, combined with their high surface areas are two advantages that would qualify biochars to be potential anode fuels for DCFCs.

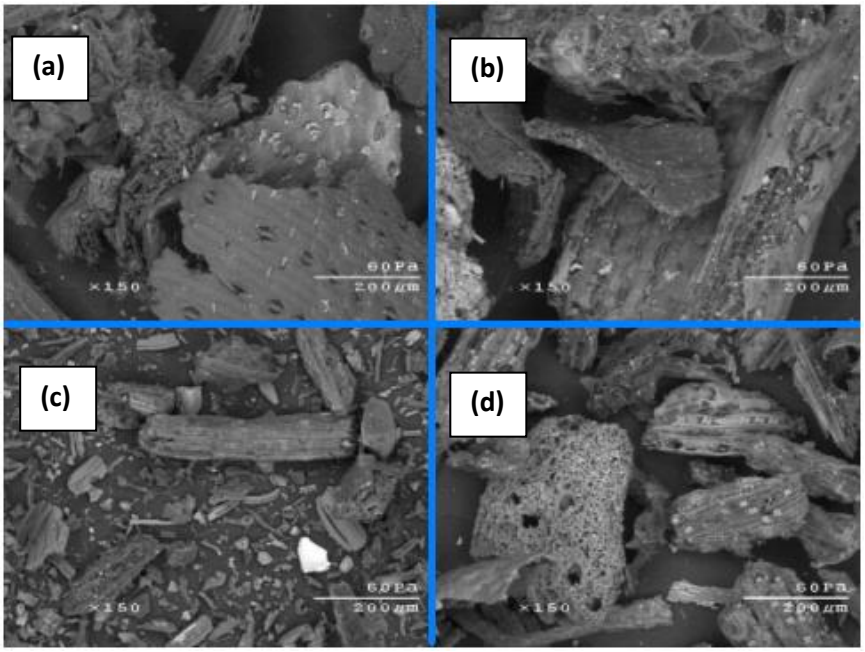

Figure 2.13: Scanning electron micrographs of switchgrass (a) feedstock, (b) slow pyrolysis char, (c) fast pyrolysis char, and (d) gasification char. (Brewer et al., 2009).

The biochar is usually a good adsorbent with a large surface area and have an electrical conductivity comparable to that of graphite (Antal and Gronli, 2003). Thus, the biochar properties are a combination of charcoal properties (large surface area with a developed porous structure) and graphite properties (good electrical conductor), which means that

biochars have a good wetting ability, high degree of reactive sites, and they good electricity conductors. These properties qualify the biochars to be potential candidates as anodefuels for DCFCs.

Inorganic compounds in the poultry litter are partially volatilized with the major proportion being retained in the structure of biochar. They are concentrated in the biochar pores due to the loss of C, H and O during pyrolysis (Lehmann and Joseph, 2009). Carbon concentrations in the biochars decrease with the increase of mineral content (ash) of the feedstock. (Gaskin et al., 2010).

The ash content of poultry litter is very high compared to other organic feedstock. That ash is a mixture of inorganic that comes from the poultry nutrients. Such inorganics may include carbonates, sulfates, and other salts. So far, these inorganics in the biochar were used as (1) soil amendment; to promote healthy plant growth by moderating the soil pH and establish a conductive structure for root growth, air exchange and water retention, and as (2) fertilizers; which are used by the plant to make proteins and carbohydrates necessary for its growth.

The idea of the present study is to evaluate those inorganics as electrical current conductors at high temperature, and to achieve that, poultry litter biochar was characterized as a potential anode for Direct Carbon Fuel Cell.

2.7 Carbonate electrolyte

2.7.1 Carbonate electrolyte for fuel cell

As highly conductive electrolytes, molten carbonates were widely used in molten carbonate fuel cells (MCFC). They were also appreciated for their suitable melting temperature, especially when they form eutectic mixtures. Kouchachvili and Ikura (2011) reported that the melting point of ternary carbonate mixtures can be further decreased by adding the right amount of carbonates or some oxides. They identified the melting point of the studied ternary carbonate mixture (43.5 mol% Li_2CO_3, 31.5 mol% Na_2CO_3, 25 mol% K_2CO_3) as 397° C, which is 100° C less than the melting point of the binary eutectic (38 mol% Li_2CO_3, 62 mol% K_2CO_3). They also studied the effect of some additives ($BaCO_3$, Cs_2CO_3, Rb_2CO_3, $MgCO_3$, $CaCO_3$, V_2O_5; CeO_2; Ag_2O, Fe_2O_3) on the melting point of the ternary carbonate.

The lowest melting point (**374° C**) was obtained for the ternary carbonate mixture with 20 wt% of caesium carbonate ($CsCO_3$).

Kojima et al. (1999) explained the effect of adding $CsCO_3$ on the melting point of carbonate mixtures as follows. The addition of caesium carbonate to carbonate mixtures increased the gas solubility and decreased the melting point by decreasing the surface tension of the molten carbonates mixture. They also concluded that the decreased surface tension of the carbonate mixtures, increases their distribution between the fuel cell components e.g. anode, cathode, and electrolyte matrix, leading to the enhancement of the DCFC performance.

Moreover, the CO_2 produced from the electro-oxidation of carbon, ensure the stability of the carbonate ions. Molten carbonates are also attractive for DCFC.

The use of molten carbonate electrolyte for direct conversion of carbon started as early as 1979, when Weaver and his team tested several types of carbon fuels. They concluded that the high reactivity of some of the carbons (devolatilized coal) with carbonate ions, is attributed to their large surface area and their low graphitic structure (Jiang and Irvine, 2011).

Vutetakis and Skidmore (1987) used stirring technique to homogenise the molten carbonate slurry where carbon particle were dispersed. They reported that the stirring approach promoted the electrochemical oxidation of carbon in the molten carbonate due to fast kinetics and mass transfer rates which resulted from stirring of the slurry with carbon particle in it. Furthermore, the stirred coal slurry overcame the anode shedding problem which had arisen with coal-derived anodes.

Chen et al. (2010) reported that pre-soaking certain percentage of the carbonate electrolyte into the anode carbon resulted in a remarkable power density improve, which is explained by the increase of the carbon-electrolyte reaction interface.

2.7.2 Challenges to face when using molten carbonate electrolytes

Carbonate electrolytes were reported to be corrosive at high temperature and as a result, the DCFC parts would experience degradation due to corrosion. Thus the DCFC wouldn't be able to operate for an extended period of time. (Cherepy et al., 2005; Cao et al., 2007).

Carbonate electrolytes strongly dissociate/evaporate (Equation 2.25) at 700° C (Cherepy et al., 2005), thus the lifetime of the fuel cell would be reduced since the electrolyte would

evaporate with time. Thus the presence of CO_2 is necessary for the stability of the carbonate ions.

$$CO_3^{2-} \leftrightarrow CO_2 + O_2 \qquad (2.25).$$

Jain et al., (2008) proposed a fuel cell which is a combination of a MCFC and a SOFC. They wanted to take advantage of the good conductivity of the molten carbonate electrolyte and use a porous solid ceramic oxide electrolyte (yttrium stabilized zirconia) to separate the anode from the cathode, which means that there is no need to circulate the CO_2. They also demonstrated that the presence of carbonate in the anode chamber can compromise between the anodic polarization at high carbon loading and sufficient carbonate for carbon wetting minimizing the corrosion problems.

References

1. Antal, Jr., M. J., Gronli, M. 2003. The Art, Science, and Technology of Charcoal Production. *Industrial engineering and chemistry research* 42: 1619-640.

2. Apelsa Guadalajara. "Apelsa Carbons: innovative products." http://www.carbonapelsa.com.mx/pages/english/activation.html

3. Baileys, R.T.; Blankenhorn, P.R. 1892. Calorific and porosity development in carbonized wood. *Wood Science.* 15: 19-28.

4. Banks, A. 1990. What's the use?. *Journal of chemical education.* 67: 1046.

5. Behrendt, F., Neubauer, Y., Oevermann, M., Wilmes, B., Zobel, N. 2008. Direct Liquefaction of Biomass: Review. *Chemical engineering technology* 31: 667–677.

6. Boateng, A. A. 2007. Characterization and Thermal Conversion of Charcoal Derived from Fluidized-Bed Fast Pyrolysis Oil Production of Switchgrass. *Industrial and engineering chemistry research* 46: 8857-8862.

7. Brewer, C. E., Schmidt-Rohr, K., Satrio, J. A., Brown, R. C. 2009. Characterization of Biochar from Fast Pyrolysis and Gasification Systems. *Environmental Progress & Sustainable Energy*. 28: 386-396.

8. Cao, D., Sun, Y., Wang, G. 2007. Direct carbon fuel cell: Fundamentals and recent developments. *Journal of Power Sources.* 167: 250–257.

9. Cao, D., Wang, G., Wang, C., Wang, J., Lu, T. 2010. Enhancement of electrooxidation activity of activated carbon for direct carbon fuel cell. *International journal of hydrogen energy* 35: 1778–1782.

10. Chen, J. P., Wu, S. 2003. Acid/Base-Treated Activated Carbons: Characterization of Functional Groups and Metal Adsorptive Properties. *Langmuir.* 20: 2233 - 2242.

11. Chen, M., Wang, C., Niu, X., Zhao, S., Tang, J., Zhu, B. 2010. Carbon anode in direct carbon fuel cell. *international journal of hydrogen energy* 35: 2732 – 2736.

12. Cherepy, N. J., Krueger, R., Fiet, K. J., Jankowski, A. F., Cooper, J. F. 2005. Direct Conversion of Carbon Fuels in a Molten Carbonate Fuel Cell. *Journal of electrochemical society* 152: A80-A87.

13. Cooper, J. F. 2005. Direct conversion of chemically De-Ashed coal in Fuel Cell (II). *Presented at 208th Electrochemical society meeting,* Los Angeles, October.

14. Cooper, J. F. 2003. Reactions of the Carbon Anode in Molten Carbonate Electrolyte. *Presented at Direct Carbon Fuel Cell Workshop*, California, July.

15. Cooper, J. F., Cherepy, N., Krueger, R. L. 2005. Tilted fuel cell apparatus. U.S. patent 6,878,479.

16. Cooper, J. F. 2007. "Direct Conversion of Coal Derived Carbon in Fuel Cells". New Delhi, India, Anamaya Publishers.

17. De la Torre, M. D. L., Guijarro, M. M. 2010. Covalent Bonds on Activated Carbon. *European journal of organic chemistry* 2010(27): 5147–5154.

18. Dicks, A. L. 2004. Molten carbonate fuel cells. *Current Opinion in Solid State and Materials Science* 8: 379 - 383.

19. Dicks, A. L. 2006. The role of carbon in fuel cells. *Journal of Power Sources* 156: 128–141.

20. Donnet, J. B., Bansal, R. C., Wang, M. J. 1993. "Carbon black". 2nd edition, Marcell Dekker, Inc. New York.

21. Gaskin, J. W., Steiner, C., Harris, K., Das K. C., Bibens B. 2010. Effect of Low-Temperature Pyrolysis Conditions on Biochar for Agricultural Use. *Transactions of the ASABE* 51: 2061-2069.

22. Giddey, S., Badwal, S. P. S., Kulkarni, A., Munnings, C. 2012. A comprehensive review of direct carbon fuel cell technology. *Progress in Energy and Combustion Science*. 38: 360-399.

23. Glugla, P. G., DeCarlo, V. J. 1982. The specific conductance of molten carbonate fuel cell tiles. *Journal of the Electrochemical Society*. 129:1745-1747.

24. Goret, J., Tremillo, B. 1967. Proprietes chimiques et electrochimiques en solution dans les hydroxides alcalins foudue 4 comportement electrochimique de quelques metaux utilises comme electrodes indicatrices. *Electrochimica Acta*. 12:1065-1083.

25. Gür, T. M., Homel, M., Virkar, A. V. 2010. High performance solid oxide fuel cell operating on dry gasified coal. *Journal of power sources.* 195: 1085-1090.

26. Haber, F. 1907. A method for generating electrical energy from coal and gaseous fuels. Austria patent 27,743.

27. Hackett, G. A., Zondlo, J. W., Svensson, R. 2007. Evaluation of carbon materials for use in a direct carbon fuel cell. *Journal of Power Sources.* 168: 111–118.

28. He, Q., Xu, Y., Wang, C., She, S., Zhou, S., Wang, R. 2012. Silane modification and characterization of activated carbon. *Adsorption* 18: 23-29.

29. Herold, C., Hérold, A., Lagrange, P.. 1996. New synthesis routes for donor-type graphite intercalation compounds. *Journal of Physics and Chemistry of Solids* 57(6): 655-662.

30. Jacques, W. W. 1896. Method of converting potential energy of carbon into electrical energy. U.S. patent 555,511.

31. Jain, S. L., Nabae, Y., Lakeman, B. J., Pointon, K. D., Irvine, J. T. S. 2008. Solid state electrochemistry of direct carbon/air fuel cells. *Solid State Ionics*. 179: 1417-21

32. Jiang, C., Irvine, J. T. S. 2011. Catalysis and oxidation of carbon in a hybrid direct carbon fuel cell. *J. Power Sources*. 196: 7318-22.

33. Kim, S. J., Park, S. J. 2001. Influence of Plasma Treatment on Microstructures and Acid–Base Surface Energetics of Nanostructured Carbon Blacks: N_2 Plasma Environment. *Journal of Colloid and Interface Science.* 244: 336–341.

34. Kojima, T.Y., Tanimoto, K., Tamiya, Y., Matsumoto, H., Miyazaki, Y. 1999. The surface tension and the density of molten binary alkali carbonate systems. *Electrochemistry*. 67: 593-602.

35. Kouchachvili, L. Ikura, M. 2011. Performance of direct carbon fuel cell. *international journal of hydrog enenergy*. 36: 10263-10268.

36. Lee, C. G., Hur, H., Song, M. B. 2011. Oxidation Behavior of Carbon in a Coin-Type Direct Carbon Fuel Cell. *Journal of the electrochemical society* 158: B410-B415.

37. Lehmann, J., Joseph, S. 2009. Biochar For Environmental Management. Earthscan Press. London, UK.

38. Li, X., Zhu, Z. H., De Marco, R., Dicks, A., Bradley, J., Liu, S., Lu, G. Q. 2008. Factors That Determine the Performance of Carbon Fuels in the Direct Carbon Fuel Cell. *Industrial & Engineering Chemistry Research.* 47: 9670–9677.

39. Mackay, D. M., Roberts, P.V. 1982. The dependence of char and carbon yield on lignocellulosic precursor composition. *Carbon* 20: 87 - 94.

40. McKee, D. W., Chatterji., D. 1975. Catalytic behaviour of alkali-metal carbonates and oxides in graphite oxidation reactions. *Carbon.* 13: 381-390.

41. Mohan, D., Pittman, C. U. Jr., Steele, P. H. 2006. Pyrolysis of Wood/Biomass for Bio-oil: A Critical Review. *Energy & Fuels* 20: 848 - 889.

42. Moreno-Castilla, C., Carrasco-Marin, F., Maldonado-Hodar, F. J., Rivera-Utrilla, J. 1998. Effects of non-oxidant and oxidant acid treatments on the surface properties of an activated carbon with very low ash content. *Carbon* 36: 145 - 151.

43. Nevskaia, D. M., Martin-Aranda, R. M. 2003. Nitric acid-oxidized carbon for the preparation of esters under ultrasonic activation. *Catalysis Letters* 87: 143-147.

44. Patton, E., Zecevic, S. 2005. Assessment of direct carbon fuel cells. EPRI report 1011496. Palo Alto, CA.

45. Predtechensky, M. R., Varlamov, Y. D., Bobrenok, O. F., Ul'yankin, S. N. 2009. Solid Hydrocarbon Conversion in a Fuel Cell with Molten Carbonate Electrolyte. *Journal of Engineering Thermophysics.* 18: 93–98.

46. Scala, F., Chirone, R., Salatino, P. 2006. Combustion and Attrition of Biomass Chars in a Fluidized Bed. *Energy & Fuels* 20: 91-102.

47. Song, W., Guo, M. 2012. Quality variations of poultry litter biochar generated at different pyrolysis temperatures. *Journal of Analytical and Applied Pyrolysis*. 94: 138-145.

48. Streubel, J. D. 2011. "Biochar: Its characterization and utility for recovering phosphorus from anaerobic digested dairy effluent". PhD thesis. (Washington State Unversity, Washington).

49. Tanimoto, K., Yanagida, M., Konjima, T., Tamiya, Y., Matsumoto, H., Miyazaki, Y. 1998. Long-term operation of small-sized single molten carbonate fuel cell. *Journal of Power Sources.* 72: 77-82.

50. Verhaert, I., De Paepe, M., Mulder, G. 2009. Thermodynamic model for an alkaline fuel cell. *Journal of Power Sources*. 193: 233–240.

51. Vutetakis, D. G., Skidmore, D. R. 1987. Electrochemical Oxidation of Molten Carbonate-Coal Slurries. *Journal of electrochemical society.* 134: 3027-3035.

52. Weaver, R. D., Leach, S. C., Bayceand, A. E., Nanis, L. Electrolyte management for the coal air fuel cell. *Presented at 16-th Intersociety Energy Conversion Engineering Conference,* New York, USA.

53. Weaver, R. D., Leach, S. C., Bayceand, A. E., Nanis, L. 1977. Direct electrochemical generation of electricity from coal. SRI International Corp, California, May.

54. Wenzl, H. F. J. 1970. "The chemical technology of wood". Academic Press. New York.

55. Wissler, M. 2006. Graphite and carbon powders for electrochemical applications. *Journal of Power Sources*. 156: 142–150.

56. Zecevic, S., Patton, E. M., Parhami, P. 2004. Carbon–air fuel cell without a reforming process. *Carbon.* 42: 1983-1993.

57. Zecevic, S., Patton, E. M., Parhami, P. 2005. Direct Carbon Fuel Cell With Hydroxide Electrolyte: Cell Performance During Initial Stage of a Long Term Operation. *Presented at 3rd International Conference on Fuel Cell Science, Engineering and Technology* Ypsilanti, Michigan, USA.

58. Zecevic, S., Patton, E. M., Parhami, P. 2005. Direct Electrochemical Power Generation from Carbon in Fuel Cells with Molten Hydroxide Electrolyte. *Chemical Engineering Community*. 192: 1655-670.

Chapter 3
Experimental

Abstract

Poultry litter (PL) is one of the most difficult wastes to dispose of due to its bad smell and the pathogen risk that it brings to the water reserve once applied as a fertilizer to lands. Poultry litter is mainly manure and wood shavings. An efficient and clean way for valorising the poultry litter is by pyrolysis. In this study, and as a first step, the American poultry litter was pyrolysed at a temperature around 450° C to maximise its percentage of carbon and ash. The Tunisian poultry litter was pyrolysed at 600° C in a downstream reactor. Physical and chemical characterization of this biochar was conducted in order to evaluate its possible use as electrode for DCFCs. Three biochars, named Black, Brown and Tunisian, were analyzed by proximate analysis, CHNS elemental analysis, ultimate analysis, Brunauer-Emmet-Teller (BET) surface area, x-ray fluorescence (XRF), x-ray diffraction (XRD), Temperature Programmed Oxidation (TPO), Temperature Programmed Desorption (TPD), Thermogravimetric analysis (TGA) and Electrical conductivity.

3.1 Introduction

Nowadays, researchers are trying to develop alternative methods of waste reduction and reuse in order to reduce the impact of animal wastes on the quality of life and the environment (2) The fast pyrolysis technology is a thermo-chemical technique that can potentially be used to convert poultry litter into value-added products such as bio-oil (23 wt%), biochar (41 wt%), and gas (36 wt%) (Kim et al., 2009). The inorganic component of poultry litter, i.e ash which range from 9% to 54% (Mante, 2008), is significantly concentrated in the biochar during pyrolysis (Agblevor et al., 2010). The ash contained in the poultry litter is a mixture of various carbonates and salts which can generate ions when molten; these ions can facilitate electrons circulation between the anode and cathode of a fuel cell. In addition to ash, poultry litter is a carbon-rich material.

The idea of using the ions generated by the poultry litter biochar at high temperature and the abundance of carbon in that biochar, motivated us to investigate the poultry litter biochar as a potential electrode for Direct Carbon Fuel Cells (DCFCs).

To ensure the reproducibility of our measurements, this chapter emphasizes the details of the experimental methods and protocols used for the preparation and characterization of the biochars.

3.2 Preparation and characterization of the biochars

3.2.1 Poultry litter selection

The poultry litter (PL) used to generate the biochar was a mixture of different poultry litters obtained from poultry farmers in Dayton, Virginia, U.S.A. Mixing the different litters was performed in a way that the ash content of the biochar, after pyrolysis, was 20 wt%. Consequently, fertilizers based on a constant-ash content-biochar will have a consistent and reproducible composition. Prior to thermochemical processing, feedstocks were ground and air-dried overnight. Before fast pyrolysis, moisture, and ash content of the PL, were determined in triplicates using ASTM proximate analysis method for wood charcoals (ASTM D1762-84).

3.2.1.1 Fast pyrolysis of the U.S.A poultry litter

Fast pyrolysis of the poultry litter blend was performed in a bench-scale fluidized bed reactor located in the Bioinnovation Center building 620 at Utah State University, Logan, UT (Figure 3.1). The pyrolysis unit comprised of a K-Tron volumetric feeder, a 50mm in diameter and 500mm in length bubbling fluidized bed reactor equipped with a 100µm porous metal gas distributer. The reactor was connected, in series, with a hot gas filter, two condensers chilled with ethylenglycol, an electrostatic precipitator, a coalescing filter and a Varian 490-Micro GC equipped with a thermal conductivity detector (TCD) and two columns (Molecular sieve 5A and a Poraplot U). The reactor was heated with a three-zone electric furnace (Thermcraft, Winston-Salem, North Carolina). 70g of sand (silica), with a particle size of 50-70 mesh was used as the fluidizing medium and the bed was fluidized with nitrogen (13L/min).

About 447g of poultry litter were pyrolyzed at 450° C. The feed rate of the feedstock was 150-200g/h. Using a screw feeder, the feedstock was conveyed from the hopper to an

entrainment zone where a 6L/min nitrogen gas was used to entrain the feed through a jacketed air-cooled feeder tube into the fluidized bed. To avoid the blockage of the feeding tube poultry litter with a particle size of 40-80 mesh was used. During pyrolysis, the mixture of vapors, gases and some of the biochar that exited from the reactor were separated by the hot gas filter maintained at 400° C to avoid the condensation of vapors going through it. The biochar particles were stopped by the hot gas filter, while the biochar-free vapors and gases passed through two condensers connected in series. These condensers were maintained at -8° C using an 18-liter Haake A82 Temperature Bath/Recirculator (Haake, Karlsruhe, Germany). The cooling liquid used for cooling is a mixture of 50/50 ethylene glycol and water.

The aerosols and non-condensable gases that escaped from the condensers passed through an electrostatic precipitator (ESP) maintained at 20 kilovolts. The ESP is made of a plastic body and a metallic rod which has electrical charges on its surface to charge the aerosol particles. The aerosol particles which have similar charge as the ESP rod are attracted to the plastic wall of the ESP body. The aerosols which escaped the ESP are trapped a F72C Series oil removing coalescing filter (NORGREN, Littleton, Colorado, U.S.A.). The clean non-condensable gases that came out of the coalescing filter passed through a totalizer which measured the total amount of gases. A sample of the non-condensable gases that came out of the coalescing filter was analysed using a Varian 490- micro gas chromatograph (GC) (Agilent Technologies Inc. California, U.S.A).

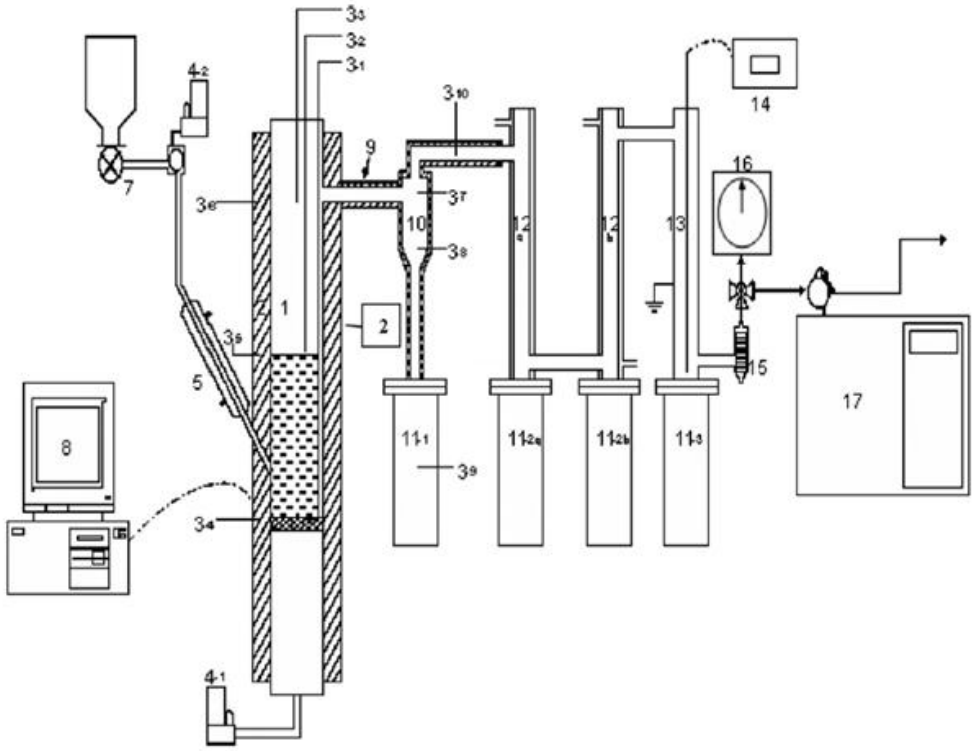

Figure 3.1: Schematic diagram of the fluidized bed reactor unit ((1) fluidized bed, (2) furnace, (3) thermocouple, (4) mass flow controller, (5) jacketed air-cooled feeder tube, (6) hopper, (7) screw feeder, (8) computer, (9) heating tape, (10) hot gas filter, (11) reservoir, (12) condenser, (13) ESP, (14) AC power supply, (15) filter, (16) wet gas meter, (17) gas chromatograph) (Agblevor et al., 2010)

After pyrolysis of the USA poultry litter, two differently coloured biochars were obtained, and they were named the Black and the Brown biochar. The brown Biochar was adsorbed on the surface of the hot gas filter. It had a particle size of 140-170 mesh (particle size: 80-100 µm) and it had a reddish brown colour, which was believed to be due to the iron (III) oxide (Fe_2O_3). The biochar, bio-oil and gas yields were 43.9 wt%, 41.9 wt% and 14.2 wt%, respectively. The biochar consisted of 80 wt % Black and 20wt % Brown biochar.

3.2.1.2 Slow pyrolysis of the Tunisian poultry litter

The poultry litter from Tunisia (poultry farmers in Sfax, Tunisia) was pyrolysed in a biomass pyrolysis pilot plant (Figure 3.2) which was made of two metallic chambers (5) where the biomass loaded to the drawers (4) is pyrolysed, the pyrolysis vapours are conducted through the pyrolysis vapors-recirculation-circuit (14) to the combustion chamber (1) which uses these pyrolysis vapours as fuel to provide heat to the pyrolysis chambers. The de-polluted combustion gases are evacuated out of the combustion chamber through a chimney (8). The pyrolysis and combustion chambers are separated by a heat exchanger (3) which transfers

heat to the pyrolysis chambers, and prevented the combustion fumes and gases from contaminating the feedstock vapours. 6 kg of poultry litter was loaded to the pyrolysis chambers (3 kg in each) and spread into a 1 centimetre layer in the drawers. After sealing the pyrolysis chambers, wood was fed to the combustion chamber through inlet (2) then put on fire to heat up the system. An electric fan was used to blow air into the combustion chamber.

It is also possible to collect bio-oil by blocking the pyrolysis vapors-recirculation-circuit (14) and let the pyrolysis vapours go through the pyrolysis vapours evacuation-tube (7). The cooled-water bath (8) ensures the condensation of the vapours which will be collected as bio-oil in the end of the vapours evacuation-tube (7). The heating was not controlled and the temperature in the feedstock chambers was measured using an electronic thermocouple (10-11).

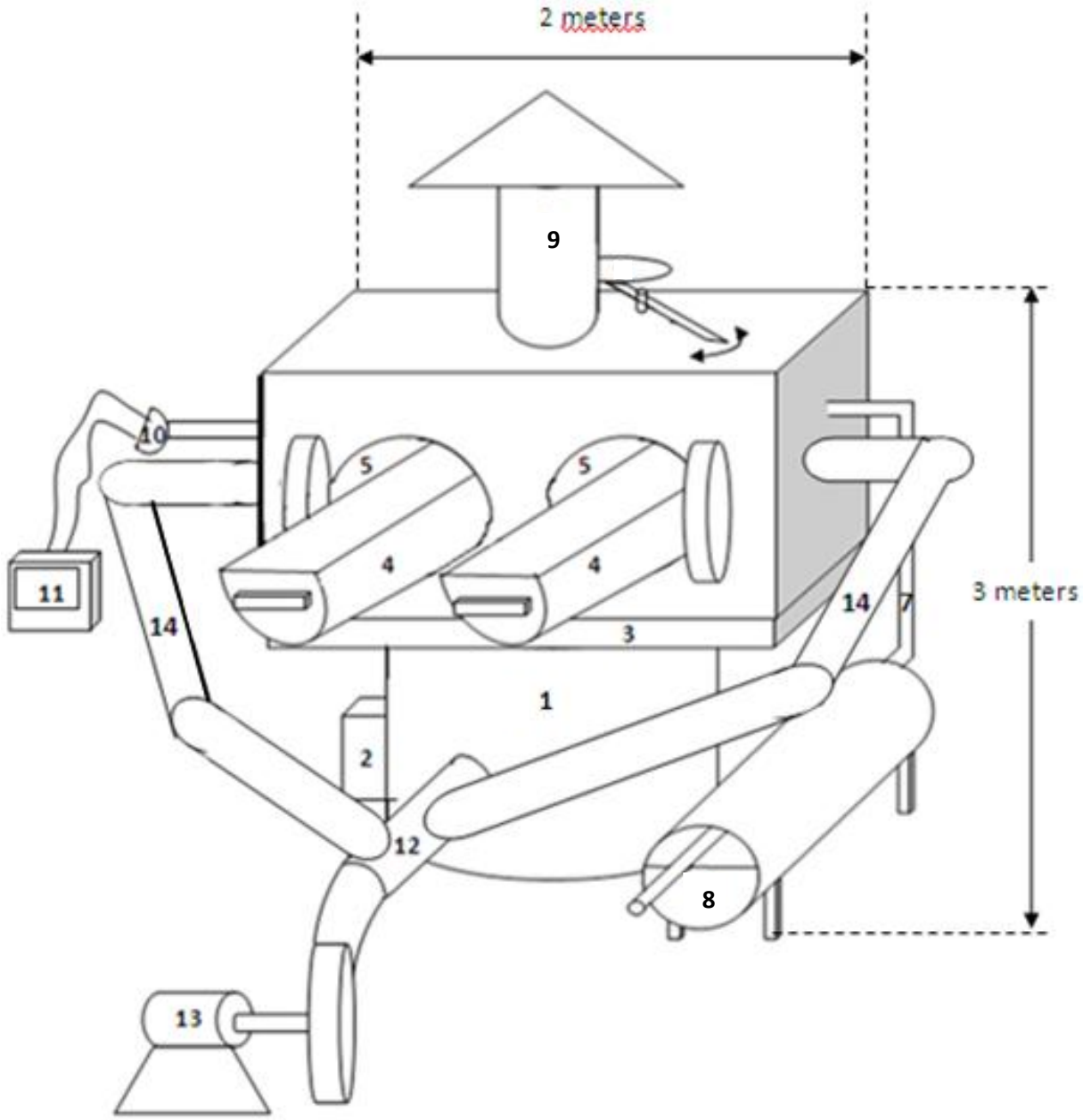

Figure 3.2: Schematic of the updraft gasifier: (1) combustion chamber, (2) combustion room wood inlet, (3) heat exchanger, (4) chambers for feedstocks loading, (5) gasification chambers, (6) vapors conducting tube, (7) pyrolysis vapours evacuation-tube, (8) cooled water bath, (9) combustion gases exhaust, (10) thermocouple, (11) temperature display screen, (12) fan air inlet, (13) electrical motor, (14) pyrolysis vapors-recirculation-circuit.

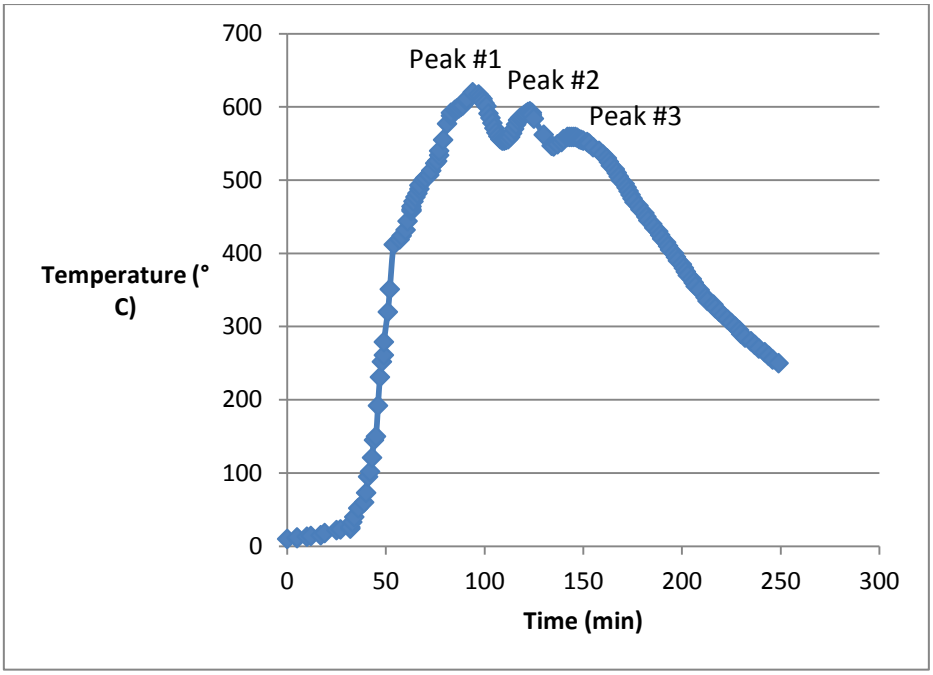

Figure 3.3: Temperature profile during the pyrolysis of the Tunisian poultry litter at 600° C.

After 83 minutes, the pyrolysis chamber temperature reached 600° C, and then started cooling down. The temperature profile of the pyrolysis chamber is shown in Figure 3.3. The temperature started increasing slowly in the pyrolysis chamber because the heat generated from the combustion chamber was used to evaporate the moisture in the poultry litter. Then, the temperature of the biomass started increasing due to its heating phase, followed by a fast thermal decomposition of cellulose and hemicelluloses (from 200 to 400° C), generating volatile matter which are sucked out of the pyrolysis chambers and injected into the combustion chamber where they were burned to generate more heat to the system. A

Starting from 400° C, a decrease in the temperature increase rate can be seen, and was due to the slow and exothermic decomposition of lignin until 600° C (peak #1). Then the temperature started decreasing. Peak #2 and Peak #3 were due to a non-continuous feeding of the combustion chamber with wood chips.

The particle size distributions of the Black, Brown and Tunisian biochar are reported in Figure 3.4. It can be seen that based on the particle size, we can order the three biochars as following Brown < Black < Tunisian.

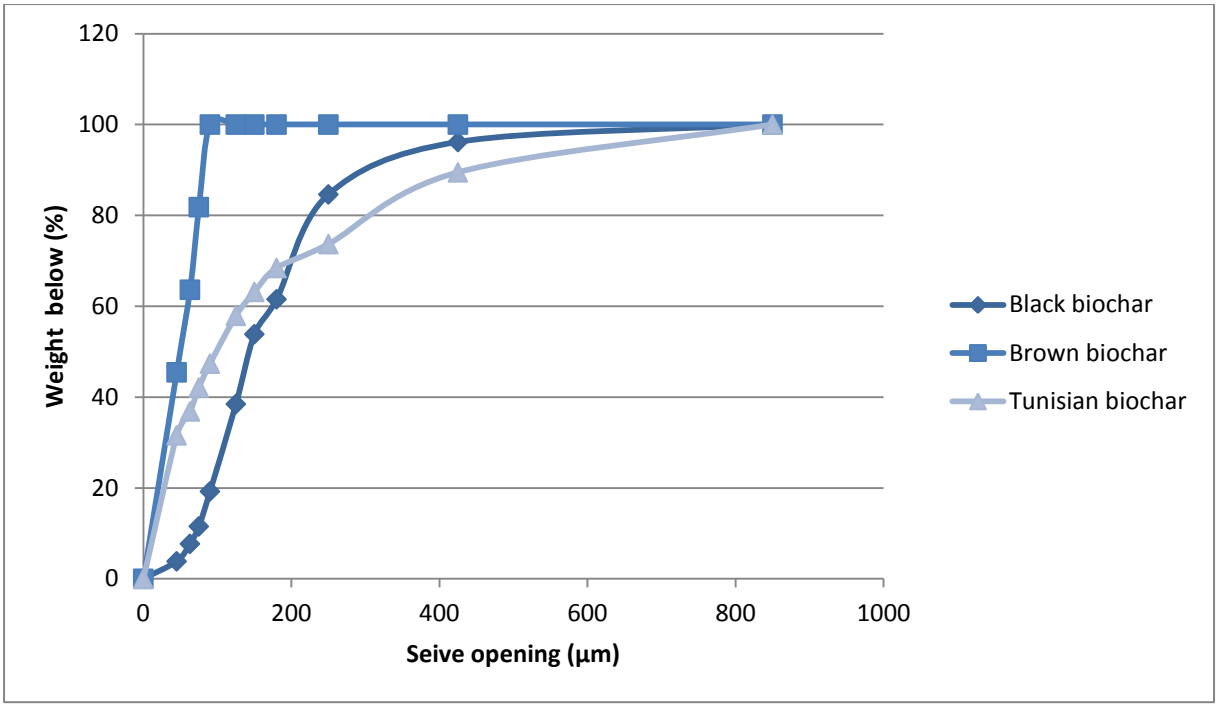

Figure 3.4: Particle size distributions of the Black, Brown and Tunisian biochars.

3.2.2 Physical and chemical characterization

3.2.2.1 X-Ray diffraction

X-ray diffraction (XRD) characterization of biochar samples was performed on a Panalytical XPert Pro XRD with Cu tube 24 KV, JADE indexing and identification software for X-ray Diffraction (Panalytical Inc., Westborough, MA, U.S.A). in the Geology Department at Utah State University in Logan, UT. The scanning rate of the analysis was 2°/min in the 2θ range from 10° to 90°. The X-ray diffraction analysis was performed for two reasons; to identify the major compounds in the three biochars, and to calculate the average crystallites size using the Debye-Scherrer equation (Equation 3.1).

$$L = \frac{K \times \lambda}{\beta \times cos\theta} \quad (3.1)$$

Where λ is the wavelength of the X-Ray, θ is the diffraction angle, K is the shape factor, and β is the peak width at half-maximum intensity. For L_c , and L_a , determination, K =0.9 and 1.84 respectively. (Radovic et al.,, 1983).

3.2.2.2 Electrical conductivity

The electrical conductivity was measured for cylindrical biochar pellets obtained by pressing 2 grams of biochar at 1990 kg/cm² (195 MPa) on a 100 ton hydraulic press. The circuit used to measure the electrical conductivity consisted of a voltage generator, multimeter, connection electrical cables and two copper electrodes with a silver paste layer on the contact surface of the biochar pellet (Figure 3.5). The silver paste was used as electron collector on the surface of the two electrodes. A schematic of the circuit is represented in Figure 3.6.

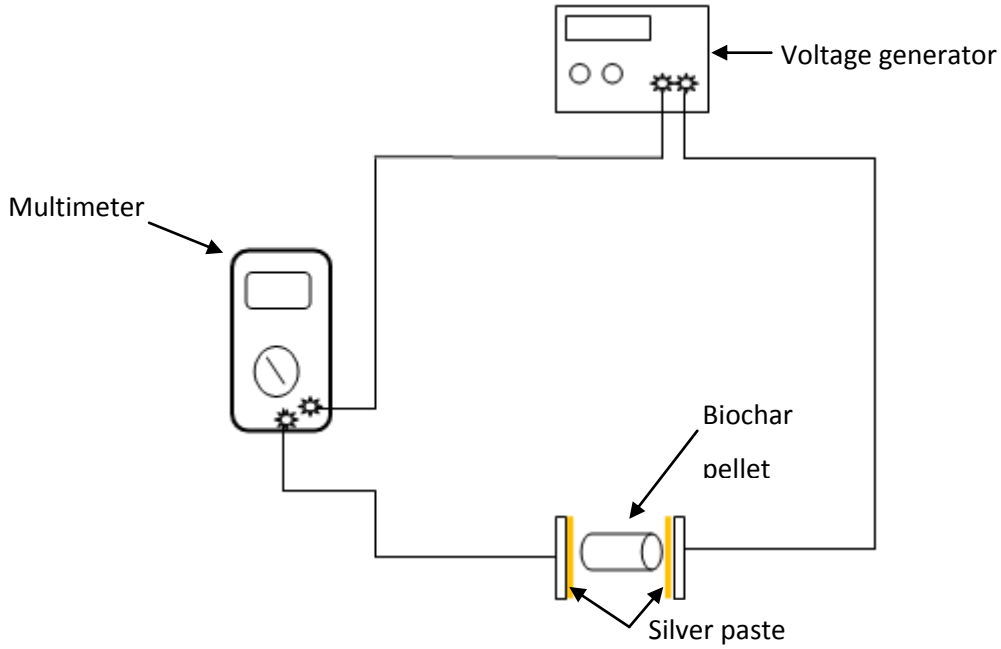

Figure 3.5: Electrical circuit used to measure the voltage and current necessary for the calculation of the electrical conductivity of the biochar samples.

The voltage (V) within the pellet as well as the current (I) going through it were measured and the resistance (R) was calculated using Ohm's law (Equation 3.2). In addition, the cross sectional area (A) and the length (l) of the pellet were measured. The resistivity (p) was measured using Equation 3.3.

$$R = \frac{V}{I} \qquad (3.2)$$

Where:

R: Resistance in ohm.

V: voltage (V)

I: electrical current (A)

$$p = \frac{R \times A}{l} \qquad (3.3)$$

Where:

R= resistance in ohm.

p=resistivity in ohm.meters

l=length of sample

A=area of the cross-section.

3.2.2.3 Nitrogen adsorption

Nitrogen (N_2) adsorption experiments were carried out in a Quantachrome Monosorb: Rapid single point B.E.T Surface analyzer (Quantachrome Instruments, Boyton Beach, FL, U.S.A) at 77 K (-197° C). Before running any test with a biochar sample, a standard (Al2O3) with a known single-point BET surface area (103.75 ± 5.33 m²/g) was used to test the accuracy of the Monosorb. Between 0.1 and 0.5g of bichar was introduced into a glass cell for degassing. All samples were degassed at 200° C for 8 hours prior to the N_2 adsorption. After degassing, the sample was weighed again then the sample cell with the biochar sample was placed into the sample station. Liquid nitrogen was used to bring the temperature of the sample cell to 77° K (~ -197° C). After adsorption, the S_{BET} was displayed on the integrator of the Monosorb.

The total pore volume (V_p) was calculated using Equation 3.4 from the manual of the Monosorb.

$$V_p = \frac{X}{\rho_{(liquid\ N_2)}}\ (cm^3) \qquad (3.4)$$

Where:

$\rho_{(liquid\ N_2)}$: density of liquid nitrogen (0.807 g/ml)

X: adsorbate weight in grams, and is calculated using Equation 3.5.

$$X = \frac{A_{sig} \times W_c}{A_{cal}} \qquad (3.5)$$

A_{sig}= surface area read on the Monosorb integrator (m^2).

W_c= the calibration gas (air) weight in grams, and it is calculated using Equation 36.

$$W_c = \frac{P_{amb}(mm\ Hg) \times M_{air}(g.mole^{-1}) \times V_c(cm^3)}{T_{amb}\ (°K) \times 760\ (mm\frac{Hg}{atm}) \times \frac{82.057(atm.cm^3)}{°K.mole}} \qquad (3.6)$$

P_{amb}: ambient barometric pressure. In Logan P_{amb}=633 mmHg

T_{amb}: ambient temperature (298 K).

V_c: the volume of air injected and which will give a surface area reading within 10% of $A_{sig.}$ (cm^3)

M_{air}: molecular weight of air (28.96 g/mol).

A_{cal}= surface area read when V_c is injected (m^2).

3.2.2.4 Thermogravimetric analysis (TGA)

Thermo-gravimetric analyses (TGA) were conducted using a TGA-Q500 (TA Instruments, New Castle, DE, U.S.A). About 10 mg biochar was loaded into a platinum pan and heated, under nitrogen atmosphere (N_2 60 ml/min), from room temperature up to 900° C at a heating rate of 10° C/min. As soon as the temperature reached 900° C, the device automatically started cooling down to room temperature. The weight of the sample was recorded after the analysis and the yield of the biochar residue was calculated. The decomposition temperatures of the major compounds were used for preliminary identification.

3.2.2.5 Temperature programmed oxidation

Temperature programmed oxidation (TPO) experiments were carried out in the TGA-Q500 in order to evaluate the relative activity of carbon oxidation assuming that the mechanism behind carbon oxidation is similar to the chemical oxidation of carbons as suggested by Vutetakis and Skidmore (1987). 10mg of biochar was loaded into a platinum pan and heated up to 200° C under N_2 atmosphere (N_2, 60°C/min) at 20° C/min, to 200°C, and held for 60 minutes to remove the adsorbed water, the temperature was further increased to 900° C in air (air, 80°C/min) at a heating rate of 10° C/min. As soon as the temperature reached 900° C, the device started cooling down to room temperature.

3.2.2.6 Temperature programmed desorption

Temperature programmed desorption (TPD) is a commonly used technique to provide the amount, stability, and nature of carbon surface oxygen complex. Between 200 and 500mg of biochar was loaded into a platinum pan, heated to 110° C, under Nitrogen atmosphere (N_2, 60 ml/min) at 10° C/min, after reaching 110° C and holding for 60 min, the temperature was further increased to 900° C in Argon (Ar, 80° C/min) at a heating rate of 5° C/min. A Varian 490- micro Gas Chromatograph (GC) (Agilent Technologies Inc. California, U.S.A), was connected to the gas exhaust of the TGA to analyse the gases evolved. The micro GC was equipped with a thermal conductivity detector (TCD) and two columns; Molecular Sieve 5 A and a Poraplot U column.

3.2.2.7 X-Ray fluorescence (XRF)

The XRF analysis is a tool used to determine the surface composition of the biochars. XRF analyses of the biochar samples were conducted in the Geology Department at USU using a Panalytical PW2400 XRF Spectrometer with 60 KV Rh tube and sample changer for X-ray Fluorescence (Panalytical Inc., Westborough, MA, U.S.A).

3.2.2.8 Elemental analysis

Organic elemental analysis was carried out using Flash 2000 Elemental Analyzer (Thermo scientific, West Palm Beach, FL, U.S.A). Before analysing any sample, standards as well as a blank, were tested on the machine. To determine the carbon, hydrogen and nitrogen in the sample, 1 mg of biochar was loaded into an aluminium container then the container was loaded to the auto-sampler to start the analysis.

In order to determine the inorganic elements in the biochars, a thermo electron Iris Advantage Inductively-coupled plasma atomic emission spectrophotometer (ICP-AES), (Thermo Fisher Scientific, Waltham MA**)** was used in the USU Analytical Laboratory, Logan, UT, U.S.A.

The method used for the sample preparation is a modification of the wet-ash method from Association of Analytical Chemists (AOAC) Method 935.13, substituting H_2O_2 for $HClO_4$ since the latter requires special hoods, and is very dangerous. 0.5g of the biochar samples were first dried at 60° C and ground to 20 mesh, then added to a digestion tube. 8 ml of concentrated nitric acid (HNO_3) was added to the biochar and after covering the tube with a watch glass, the mixture was heated to 95° C for one hour in a digestion block, then allowed to cool down for approximately 15-20 minutes. After adding 4 ml of 30% hydrogen peroxide (H_2O_2), the mixture was placed again in the hot (95° C) digestion block for 30 minutes then the sample tube was cooled for 30 minutes to avoid foaming/fizzing. Two more additions of 4 ml of H_2O_2 followed by heating at 95° C for one hour were carried followed by cooling for 15-20 minutes. Finally, the sample mixture was brought to a 25 ml final volume with deionized water.

References

1. Agblevor, A. F., Beis, S., Kim, S. S., Tarrant R., Mante, N. O. 2010. "Biocrude oils from the fast pyrolysis of poultry litter and hardwood." *Waste Management* 30: 298-307.

2. Huang J., Yang L., Gao R., Mao Z, Wang C. (2006). "A high-performance ceramic fuel cell with samarium doped ceria–carbonate composite electrolyte at low temperatures." *Electrochemistry communications* 8: 785-789.

3. Jia L., Tian Y., Liu Q., Xia C., Yu J., Wang Z., Zhao Y., Li Y. 2010. "A direct carbon fuel cell with (molten carbonate)/(doped ceria) composite electrolyte." *Journal of Power Sources* 195: 5581-5586.

4. Kim S. S., Agblevor F. A., Lim J. 2009. "Fast pyrolysis of chicken litter and turkey litter in a fluidized bed reactor." *Journal of Industrial and Engineering Chemistry* 15: 247-252.

5. Li X., Zhu Z. H., De Marco R., Dicks A., Bradley J., Liu S., Lu G. Q. (2008). "Factors That Determine the Performance of Carbon Fuels in the Direct Carbon Fuel Cell." *Industrial and Engineering Chemistry Research* 47: 9670-9677.

6. Lima I. M., Marshall, W. E. 2005. "Granular activated carbons from broiler manure: physical, chemical and adsorptive properties." *Bioresource Technology* 96: 699-706.

7. Mante, N. O. D. 2008. "Influence of wood on the pyrolysis of poultry litter". Master thesis (Virginia Polytechnic Institute and State University, Blacksburg).

8. Radovic L. R., Walker P. L., Jenkins R. G. and Jenkins J. R. G. 1983. "Importance of carbon active sites in the gasification of coal chars " *Fuel* 62: 849-856.

9. Vutetakis D. G., Skidmore D. R. (1987). "Electrochemical Oxidation of Molten Carbonate-coal slurries." *The Electrochemical society* 134(12): 3027-3035.

10. Yamada S., Fujiwara M., Kanda M. 1995. "Synthesis and properties of LiNiO2 as cathode material for secondary batteries ". *Journal of Power Sources* 54: 209-213.

Chapter 4
Characterization of the biochars

Abstract

The biochars obtained from the pyrolysis of the Tunisian and the American poultry litter are composed of carbon and minerals. Identifying the mineral composition of each of the biochars will help predict their behaviour at high temperature. Physical characterization included nitrogen adsorption, X-ray diffraction, and electrical conductivity measurements. Chemical characterization included Inductively-coupled plasma spectrometry, thermo-gravimetric analysis, X-ray fluorescence, temperature programmed oxidation (TPO), and temperature programmed desorption (TPD). The ash and fixed carbon content were respectively 47 wt% and 22 wt% in the Black biochar; 63 wt% and 19 wt% in the Brown biochar; and 32.5 wt% and 35 wt% in the Tunisian biochar. The ashes of the PL biochars contain between 40.25 and 43.08 wt% catalytic oxides (CaO, MgO, K_2O and Fe_2O_3) for carbon oxidation, and between 3.21 and 6.62 wt% inhibitor oxides (Al_2O_3, SiO_2, and Ti_2O) for the anode. The PL biochars had a low average optimal burn-off temperature of 438.75° C which was a result of their highly disordered structure and high content of carbon-oxidation catalytic oxides. At room temperature, all three biochars have a very low (negligible) electrical conductivites i.e. $70.56x10^{-9}$ $S.cm^{-1}$, $12.15x10^{-9}$ $S.cm^{-1}$, and $7.7x10^{-9}$ $S.cm^{-1}$ for Black, Brown and Tunisian biochars, respectively. Compared to charcoal, the low BET surface areas and the limited pore volumes of the Black (4.20 m^2/g and $17.25x10^{-4}$ cm^3/g), the Brown (3.2 m^2/g and $12.87x10^{-4}$ cm^3/g), and the Tunisian biochar (3.88 m^2/g and $18.39x10^{-4}$ cm^3/g) may be due to the occupation of the pores and surfaces of the biochars by mineral compounds. The low fixed carbon contents, the negligible electrical conductivities, the low surface areas and the high ash contents, disqualified PL biochar (as they are) from being potential anode fuels for DCFCs.

4.1 Introduction

In order to determine whether the PL biochar can be a potential fuel for DCFCs, a thorough understanding of the biochar chemical and physical properties is necessary. In addition to that, a comparison between the PL biochars properties and those of some carbon materials (reported in the literature) such as commercial carbons (graphitic carbon, activated charcoal and carbon black) and coals (Germancreek, Blackwater) (Li et al., 2008; Li et al., 2010b), was conducted in order to understand the possible effect of biochar properties on the operation of DCFC.

4.1 Thermo-gravimetric analysis of the biochars

Thermo-gravimetric analyses were used for preliminary identification of the major compounds within the biochars. The thermal decomposition of volatile compounds under inert atmosphere (e.g. nitrogen) can occur until 950° C. Thus, the remaining matter is made of fixed carbon and ash. Therefore, the TGA analysis under inert atmosphere will identify the temperature range of the thermal decomposition of the volatiles in the PL biochars.

The experiments were carried using TGA-Q500 analyzer (TA Instruments, New Castle. DE. U.S.A). Figure 4.1 a-c, shows the different TGA profiles generated for the Black, Brown, and Tunisian biochars.

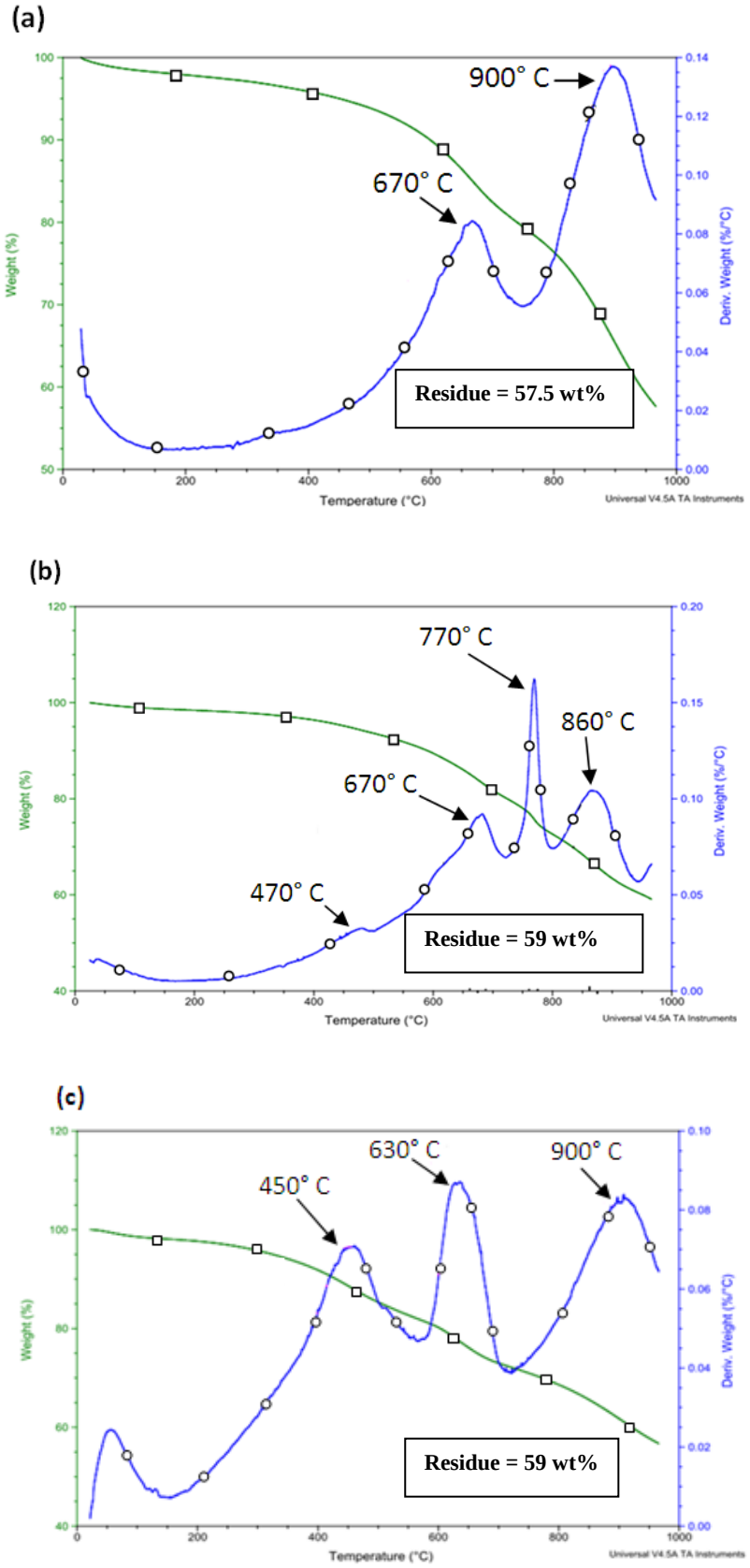

Figure 4.1 : TGA (-□-) and DTG (-○-) profiles describing the weight loss vs. Temperature for (a) the Black, (b) the Brown, and (c) the Tunisian biochars.

For all samples, it can be seen that there is a small weight loss below 100° C attributed to the desorption of physisorbed water (Li et al., 2008; Marinov et al., 2010). The Black, Brown, and Tunisian biochars had moisture content of 3.5 wt%, 2.6 wt%, and 5 wt%, respectively.

The volatile matter decomposition/volatilization for the Black (Figure 4.1-a) and Brown (Figure 4.1-b) biochars started slowly at 300° C until 500° C, and then an intense volatile matter release was observed at higher temperature (from 500° C to 750° C). The temperature of maximum volatile matter release was 670° C for both biochars. The slow mass losses between 300 and 500° C was maybe due to the decomposition of the side groups with low thermal stability such as carboxyl groups (This is contradicting the CO_2-TPD analysis since the Black and Brown biochars didn't produce a lot of CO_2 between 500 and 750° C), followed by the splitting-off of the more resistant side groups (e.g. lactone) and the formation of aromatic rings. The intense volatile matter release from 500 until 750° C was attributed to the decomposition of the heat resistant heteroaromatic structures and the formation of polyaromatic structures (Varhegyi and Szabo, 2002). The decomposition of calcium carbonate ($CaCO_3$) to CaO and CO_2 may also have contributed to the weight loss between 600° C and 700° C. Calcium carbonate is fed continuously to the poultry to help the formation of egg shells.

The DTG profile of the Brown biochar exhibited two more decomposition/devolatilization peaks that were not observed for the Black biochar. The first DTG weak peak (shoulder) at $T_{50\%}$ = 470° C was attributed to the dehydroxylation of $Mg(OH)_2$ (Khan et al., 2001). The second DTG peak at $T_{50\%}$ = 770° C may be attributed to the volatilization of KCl (Alfieri et al., 2012). In fact, the Brown biochar was adsorbed onto the hot gas filter porous surface through which a mixture of gases (N_2, CO_2, CO, H_2O, O_2 and other gases) was continuously flowing, and the temperature of the hot gas filter was maintained between 450 and 500° C. Under these conditions KCl and SiO_2, formed an agglomerate with the chemical formula $K_2Si_4O_9$ (Gatternig et al., 2010; Geisinger et al., 1987) in which, SiO_2 fine particles were a KCl-crystals support. The devolatilization of KCl crystals was a possible explanation for the distinguished peak at 770° C present in the DTG profile of the Brown biochar but not on the DTG of the Black biochar, even though they were obtained from the same poultry litter.

The last DTG peak for both the Black and Brown biochars at $T_{50\%}$ = 900 and 860° C, respectively, was attributed to the decomposition of calcium carbonate ($CaCO_3$) (Skreiberg et al., 2011; Jung et al., 2011; Alfieri et al., 2012) and the dehydroxylation of talk

($Mg_3Si_4O_{10}(OH)_2$), which occur between 650 and 1000° C (Belgacem et al., 2008). Calcium carbonate is fed continuously to the poultry to help the formation of egg shells. Talc is used for easier broadcasting on litter beds in poultry farmes (Som Phytopharma INDIA Ltd., INDIA).

The resolution of DTG peaks of the Brown biochar was better than that of the Black biochar. This better resolution was maybe due to the fine particle size of the Brown biochar (Figure 3.4), which would allow the volatile compounds to absorb the heat faster, thus devolatilized quicker and separated from each others.

The Tunisian biochar (Figure 4.1-c) started an intensive weight loss earlier i.e. 180° C until 560° C and faster than the other two biochars (Black and Brown biochars). As mentioned in chapter three, the Tunisian poultry litter was pyrolysed as received (large pieces). Therefore, the core of the large feedstock pieces didn't receive enough heat (heat transfer limitation) to liberate the volatile matter during its pyrolysis. However, the Tunisian biochar was ground to fine particles before the TGA experiments. The fine particle size resulted in a larger surface area and the volatile matter located in the core of the biochar particles had more chances to absorb the heat and decompose/volatilize. Moreover, the decomposition of the side groups with low thermal stability such as carboxyl groups, and later the splitting-off of the more resistant side groups such as lactones and the formation of aromatic rings, may have contributed to the weight loss of the Tunisian biochar between 300 and 500° C. Another DTG peak at $T_{50\%}$ = 630° C in the Tunisia PL biochar profile, was attributed to the decomposition of the heat resistant heteroaromatic structures and the formation of polyaromatic structures (Varhegyi and Szabo, 2002). The last DTG peak was similar to the last DTG peak of the Black biochar and, therefore, was be attributed to the decomposition of $CaCO_3$ and the dehydroxylation of talc.

The residues of the three biochars were 57.5 wt%, 59 wt%, and 57 wt% for the Black, the Brown, and the Tunisian biochars. These residues included fixed carbon and ash (mineral matter). Consequently, the fixed carbon content of the three PL biochars was apparently less than 50 wt%, which was a first sign of a non potential carbon fuel for a DCFC.

Another analysis of the biochars, after leaching them with water under continuous stirring for 24 hours followed by drying overnight at 105° C, was made in order to see if some of the inorganics in the biochars were soluble in water. The TGA of the leached biochars is presented in Figure 4.2 a-c.

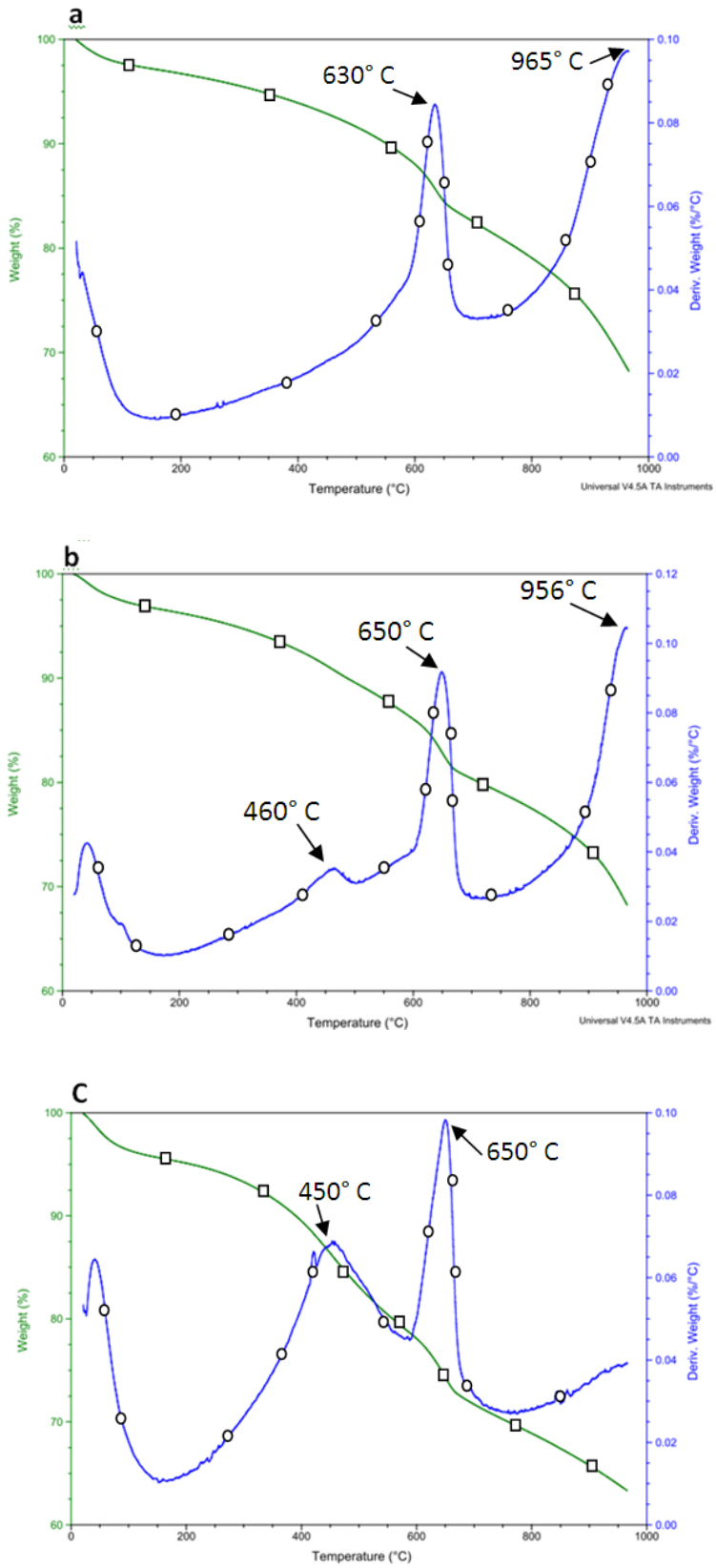

Figure 4.2 : TGA (–□–) and DTG (–○–) profiles of the (a) Black. (b) Brown and (c) Tunisian biochars, after water extraction.

Similar water desorption peaks to the previous TGA analysis were observed for the three biochars i.e. 3.5 wt%, 2.6 wt%, and 5 wt% for the Black, the Brown, and the Tunisian biochars.

It can be noticed that the DTG peaks of the Black (Figure 4.2-a) and the Brown (Figure 4.2-b) biochars became narrower compared to the previous TGA test (Figure 4.1 a-b), which indicates the dissociation of the soluble compounds. The DTG profile of the Black biochar conserved the two major peaks with some minor changes. The first peak ($T_{50\%}$=630° C) was narrowed and shifted by 40° C toward lower temperatures, whereas the last peak was shifted by 65° C toward higher temperatures. The shifting of the two peaks may be due to the dissolution of impurities that were affecting the thermal behaviour of the compounds corresponding to those two peaks i.e. (1) splitting-off of the more resistant side groups (e.g. lactone) and the formation of aromatic rings, and (2) dehydroxylation of talc and decomposition of $CaCO_3$. Another explanation of the shifting of the DTG peaks is the interfacial interaction of the inorganic mineral and the organic substrate (Wang et al., 2006).

For the Brown biochar, the DTG peak at $T_{50\%}$ = 770° C disappeared after the leachate test, which confirms that is corresponded to KCl volatilization. Moreover, the DTG shoulder at $T_{50\%}$ = 470° C (TGA test) became a peak at $T_{50\%}$ = 460° C confirming that it corresponded to the dehydroxylation of a non-soluble compound i.e. $Mg(OH)_2$ (Khan et al., 2001).

The first peak on the DTG profile of the Tunisian biochar (Figure 4.2-c) was not affected by the leaching test. The sample started an intensive weight loss earlier i.e. 150° C until 560° C and faster than the other two biochars, probably due to the decomposition of the side groups with different thermal resistance as explained previously. The DTG peak at $T_{50\%}$ = 650° C was shifted by 20°C probably due to the elimination of impurities. This peak was attributed to the decomposition of the heat resistant heteroaromatic structures and the formation of polyaromatic structures as explained previously. The last peak at $T_{50\%}$ = 900° C was attenuated by 10 wt% which was probably due to the dissociation of soluble compounds. The DTG peak corresponding to the decomposition of $CaCO_3$ was not present in Figure 4.4-c) and could be shifted toward higher temperatures, since the weight loss was still progressing until 950° C (Figure 4.4-c).

It was clear that the dissolution of impurities increased the rate of the decomposition of the heat resistant heteroaromatic structures and the formation of polyaromatic structures (at a slightly higher temperature i.e. $T_{50\%}$= 650° C) but didn’t have an effect on the decomposition

temperature ($T_{50\%}$=450° C) or rate of decomposition of the side groups with low thermal stability such as carboxyl groups.

The TGA analyses of the three PL biochars showed that the weight loss of the samples didn't stabilize up to 950° C, which indicates the presence of inorganic salts that starts decomposing after 650° C, which is a valuable information for the conduction of the proximate analysis. Moreover, the residual mass of the three biochars, after TGA analysis, was around 60 wt%, which indicated the low fixed carbon content (< 60 wt%) in the three samples since the residues contain fixed carbon + ash and the ash content of poultry litter was reported to be higher than 20 wt% (Mante and Agblevor, 2010).

4.2 Chemical composition of the biochars

The chemical composition of the three biochars is very important for their characterization since it will help to identify the different compounds and explain what is behind the behaviour of the biochars when exposed to different experimental conditions such as high temperature and the presence of oxidant species. First, proximate analyses of the three biochars were conducted in order to quantify the moisture, volatiles, fixed carbon, and ash. After that, inductively-coupled plasma spectrophotometry (ICPS) analyses were conducted for the three biochars in order to determine their precise elemental composition. Finally, the X-ray fluorescence analyses were conducted to quantify the different oxides present in the biochars.

The TGA was used to investigate the approximate analysis of the biochars. The samples were heated from room temperature until 200° C under nitrogen atmosphere (80° ml/min) at a heating rate of 20° C/min, and the temperature was held at 200° C for 60 min to allow the desorption of water from the biochars. Under nitrogen, the sample was heated from 200 to 950° C at a rate of 50° C/min, and held at 950° C for 20 min to make sure that all volatiles were separated from the sample. Then, the gas purge was switched from nitrogen to air (80 ml/min) at 950° C. The fixed carbon burned rapidly leaving ash in the TGA pan.

Table 4.1: Proximate analysis of the poultry litter biochars by TGA

PL biochars	Moisture (wt%)	Volatile matter (wt%)	Fixed carbon (wt%)	Ash (wt%)
Black	3.5	27.5	22	47
Brown	2.6	15.4	19	63
Tunisian	5	27.5	35	32.5
Coal GK*	1.2	19.6	73.4	5.8
Coal BW*	1.1	32.7	59.8	6.4

* Li et al. 2010.

The proximate analysis of the three biochars is reported in Table 4.1. The moisture content in the Black, Brown, and Tunisian biochar samples was 3.5 wt%, 2.6 wt%, and 5 wt%, respectively. It can be seen that all three biochars have low fixed carbon content (19-35 wt%) and high ash content (32.5-63 wt%). The Tunisian biochar had the highest fixed carbon content (35 wt%) and the lowest ash content (32.5 wt%) which is due to its preparation conditions (slow pyrolysis).

The ashes of the three biochars contain their mineral matter, and high ash content indicates high mineral content. Some metals (Li, Na, K, Ca, Mg, Fe, etc) and their oxides were reported as active catalysts for the carbon oxidation reactions (Marsh and Reinoso, 2005). The concentration, dispersion and chemical form of the mineral matter highly affect their catalytic activity (Speight, 1994). Therefore, Inductively-coupled plasma spectrophotometry was used to determine the elemental composition of the biochars. This method gives a precise analysis of the amount of each element present in the biochar. The elemental composition of the ash is shown in Table 4.2.

Compared to the coal samples, it can be seen that the fixed carbon content of PL biochars is very low compared to the coal samples. Moreover, the ash content of the coals is much lower than the PL biochars. The fixed carbon content is a crucial parameter for DCFC performance i.e. low fixed carbon content would result in a low carbon loading for the anodic reaction in the DCFC. Therefore, the low fixed carbon content of PL biochars is a limitation for qualifying them as potential fuel for DCFCs.

Table 4.2: Elemental analysis of the Black, Brown, and Tunisian biochars.

		Black	Brown	Tunisian
Content wt%	C	37.6	22.8	45.2
	H	1.46	1.17	2.54
	N	3.03	2.51	2.57
	O	33.9	46.06	34.32
	Ca	5.58	5.91	5.4
	K	7.53	8.03	4.88
	Mg	1.77	2.6	0.92
	P	3.61	4.5	2.14
	S	1.89	2.91	0.61
	Na	2.14	1.56	0.83
	Fe	0.38	0.55	0.14
	Al	0.35	0.55	0.07
	Si	0.27	0.38	0.17
	Mn	0.16	0.16	0.09
	Zn	0.15	0.13	0.06
	Cu	0.14	0.12	0.02
	B	0.017	0.015	0.01
	Sr	0.008	0.009	0.018
	Ni	0.006	0.016	0.0017
	Ba	0.005	0.005	0.01
	Mo	0.004	0.007	-
	As	0.002	0.003	-
	Cr	0.0008	0.0014	0.0028
	Co	0.0009	0.0008	0.0003

All three biochar samples comprise between 12.17 and 18.65 wt% of alkali metals (K and Na), alkaline earth metal (Ca and Mg) and transition metal (Fe). The amounts of aluminium and silicon are between 0.24 and 0.62 wt%. The absence of chlorine is in disagreement with the literature (Mante and Agblevor, 2010), which may be due to the calibration of the analysis machine.

Table 4.3: XRF analysis of the Black, Brown and Tunisian biochars compared to coal samples.

	Ash compositions	Black (wt%)	Brown (wt%)	Tunisian (wt%)	Coal GK* (wt%)	Coal BW* (wt%)
Content (wt%)	CaO	19.113	16.747	20.695	0.13	0.38
	P_2O_5	19.352	19.794	12.126	0.11	0.18
	K_2O	10.081	13.312	13.693	0.04	0.07
	MgO	7.26	9.441	5.451	0.02	0.09
	SiO_2	3.636	4.996	2.571	3.38	3.31
	Na_2O	2.599	2.281	1.581	0.05	0.06
	Fe_2O_3	1.196	1.299	0.611	0.23	0.63
	Al_2O_3	1.114	1.622	0.639	1.49	1.45
	MnO	0.491	0.412	0.312	-	-
	TiO_2	0.122	0.168	0.048	0.1	0.06

* Li et al. 2010.

Table 4.3 reports the results of the X-Ray fluorescence (XRF) analysis, which quantified the major and minor oxides present in the three biochars. It can be noticed that the sum of all oxides doesn't give 100% and that was due to two factors; (1) the XRF analyses were conducted using the biochar samples and not ash, so the organic elements contribution to the total mass was not counted, (2) and due to the calibration method and the samples' nature, the overall mineral content in the three biochars is overestimated, however, the relative concentrations of the elements are accurate.

All three samples comprise between 40.25 and 43.08 wt% of mineral matter in form of CaO, K_2O, Na_2O, MgO, and Fe_2O_3, and between 3.21 and 6.618 wt% of mineral matter in the form of SiO_2 and Al_2O_3.

MgO, CaO, Na_2O, K_2O and Fe_2O_3 were considered as active catalysts for the anodic reaction, while Al_2O_3, SiO_2, and TiO_2 had an inhibitory effect that decreased the performance of the DCFC (Li et al., 2010b; Vuteutakis and Skidmore, 1987). However, the catalytic activity of the mineral matter is highly dependent on their concentration, dispersion, chemical form and stability in the coal (carbon) matrix (Speight, 1994).

By contrast to the results reported by Li and co-workers (2010), coal samples named Germancreek (GK) and Blackwater (BW) contain between 0.47 and 1.23 wt% of catalytic

minerals and between 4.97 and 4.82 wt% of inhibitory minerals, respectively. When tested on DCFC, GK gave similar performance as activated carbon. Therefore, and due to the high amount of catalytic minerals, the ash of PL biochars can be considered as a natural catalyst for the oxidation reaction of the biochars.

CaO and MgO are refractory oxides (stable at high temperatures) and they are good insulators due to their very low electrical conductivities even at high temperatures i.e. 10^{-8} S/cm at 780° C for CaO and 10^{-10} S/cm at 780° C for MgO (Wilson, 1981). Therefore, the presence of these oxides would reduce the electrical conductivities of PL biochars.

4.3 Graphitic structure of the biochars

The X-ray diffraction patterns of the three PL biochars are shown in figure 4.3 A-C. It is clear that the three biochars contain a significant amount of minerals which is reflected by the numerous diffraction peaks corresponding to the different minerals present in the biochars. Amorphous carbon also contributed to the background intensity (Li et al., 2008; Lu et al., 2001; Lin and Guet, 1990). Moreover, the three biochar samples contain a broad (002) diffraction peaks at around 29° and another weak and broad (100) diffraction peak at around 45°. These two peaks indicate that the three biochars contain turbostratic structure (or graphite like structure) (Manoj et al., 2012).

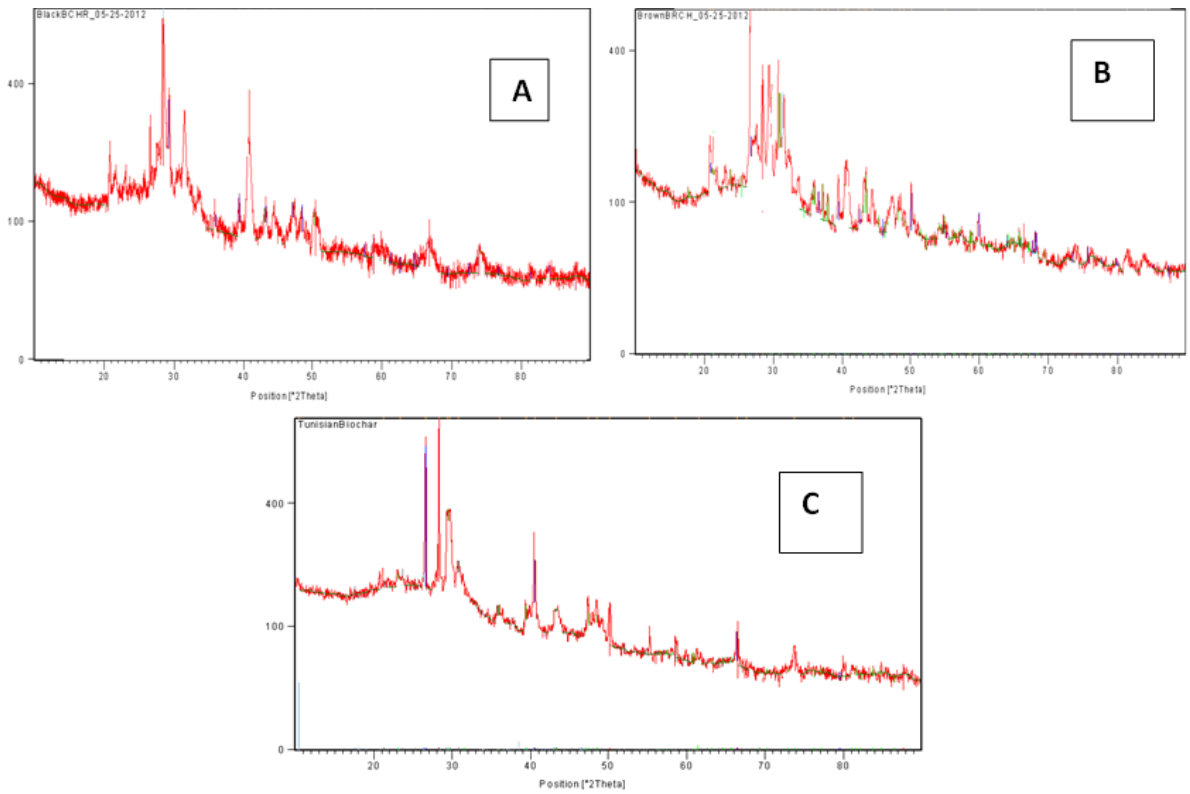

Figure 4.3: XRD patterns of the (A) Black, (B) Brown and the (C) Tunisian biochar.

Quantitative estimations of the crystalline parameters of the biochars are shown in Table 4.4, including the inter-planar distance (d_{002}), the crystallite height (L_c), and the crystallite diameter (L_a). The values of the different crystallite parameters are similar for the three biochars e.g. 3.14-3.35 Å, 10.34-10.38 Å, and 21.13-21.22 Å for d_{002}, L_c, and L_a, respectively, which indicates that the difference in crystalline structure of the three biochars is negligible, and cannot be correlated with their electrochemical reactivities.

Compared to coal samples (GK and BW) the industrial carbon i.e. activated carbon, carbon black, and graphitic carbon, PL biochars have the lower L_c and L_a, thus more disordered structure (Li et al., 2008).

Table 4.4: Crystalline parameters of the Black, Brown, and Tunisian biochars.

Biochar	XRD			Electrical conductivity (S/cm)
	d_{002} (Å)	Lc (Å)	La (Å)	
Black biochar	3.14	10.38	21.22	$70.56x10^{-9}$
Brown Biochar	3.35	10.34	21.13	$12.15x10^{-9}$
Tunisian Biochar	3.15	10.37	21.20	$7.7x10^{-9}$
Activated carbon[a]	3.73	10	45	0.8
Carbon black[a]	3.63	17	35	1.5-1.8
Graphitic carbon[a]	3.36	183	94	10.5
Coal GK[b]	3.54	16	25	-
Coal BW[b]	3.58	13	23	-

a: Li et al. (2008).
b: Li et al. (2010).

In addition to the structural analysis of the biochar samples, the raw data of XRD analysis (e.g. interplanar spacing and the diffraction angles) were investigated in order to identify the inorganic compounds found in threebiochars. Table 4.5 represents a comparison of the d-spacing values obtained from the biochars analyses, to the d-spacings in the literature. Potassium sulfate (K_2SO_4), calcium carbonate ($CaCO_3$), magnesium carbonate ($MgCO_3$), Silicon oxide (SiO2), and potassium chloride (KCl) were identified in the three biochars. The presence of chlorine (Cl) is in agreement with the literature. The XRD results are in agreement with the explanation of the origins of the different peaks in the thermogravimetric analyses. The characteristic reflections of potassium carbonate (K_2CO_3) and sodium carbonate (Na_2CO_3) were not present in the XRD pattern.

Table 4.5: Common components detected by XRD in the Black, Brown, and Tunisian biochar.

	d-spacing (Å)																			
	$CaCO_3$					K_2SO_4				$MgCO_3$					KCl				SiO_2		
	3.87[a]	3.04[a]	2.84[a]	2.50[a]	2.29[a]	3.93[b]	3.09[b]	2.10[b]	1.69[b]	2.74[c]	2.51[c]	2.10[c]	1.94[c]	1.70[c]	3.15[d]	2.22[d]	1.82[d]	1.57[d]	3.34[e]	4.26[e]	1.82[e]
Black	3.87	3.04	2.84	2.50	2.29	3.87	3.13	2.09	1.60	2.67	2.50	2.09	1.92	1.60	3.13	2.22	1.82	1.56	3.35	4.27	1.82
Δd	0.00	0.00	0.00	0.00	0.00	0.06	-0.04	0.01	0.09	0.07	0.01	0.01	0.02	0.10	0.02	0.00	0.00	0.01	-0.01	-0.01	0.00
Brown	3.87	3.04	2.84	2.49	2.28	3.87	3.04	2.09	1.67	2.76	2.49	2.09	1.92	1.67	3.14	2.22	1.82	1.54	3.35	4.27	1.82
Δd	0.00	0.00	0.00	0.01	0.01	0.06	0.05	0.01	0.02	-0.02	0.02	0.01	0.02	0.03	0.01	0.00	0.00	0.03	-0.01	-0.01	0.00
Tunisian	3.81	3.04	2.90	2.49	2.28	3.81	3.04	2.08	1.66	2.90	2.49	2.08	1.91	1.66	3.15	2.23	1.82	1.57	3.35	4.20	1.82
Δd	0.06	0.00	-0.06	0.01	0.01	0.12	0.05	0.02	0.03	-0.16	0.02	0.02	0.03	0.04	0.00	-0.01	0.00	0.00	-0.01	0.06	0.00

a: Wei et al., (2003).
b: De vries and Gallings (1969)
c: Bankauskaite and Baltakys (2011)
d: West (1999)
e: Ulery and Drees (2008)

4.4 Electrical conductivity of the biochars

The performance of the DCFC is known to be highly affected by the electrical conductivity of the carbon fuel, since the latter will ensure the electron transfer to the current connector, in addition to being consumed as the anode fuel (Li et al., 2008; Joseph et al. (2007). Moreover, carbons with high electrical conductivity (at room temperature) may reduce the ohmic polarization and improve the fuel cell performance. The electrical conductivity of the carbon material is directly related to its degree of graphitic structure. Usually, a higher graphitic degree implies a higher electrical conductivity (Li et al., 2008). The electrical conductivities of the Black, the Brown and the Tunisian biochars at room temperature are represented in Table 4.4. As expected, the Black, Brown, and Tunisian biochars had very low electrical conductivities i.e. 70.56×10^{-9} $S.cm^{-1}$, 12.15×10^{-9} $S.cm^{-1}$, and 7.7×10^{-9} $S.cm^{-1}$, respectively, because of their very low graphitic structure.

In addition to their highly disordered crystalline structure, the extremely low conductivity of the poultry litter biochars can be explained by the presence of the different inorganic compounds ($CaCO_3$, SiO_2, etc) within these materials. Table 4.6 shows what was reported in

the literature about the variation of the electrical conductivity of the different inorganics present in the three biochars with respect to temperature, charcoal was considered also since the poultry litter biochars are mainly charcoal (lignocellulosic material in the litter comes from the undigested food and the bedding of the poultry) and inorganics. With such very low electrical conductivities, the inorganics would critically decrease the electrical conductivity of the PL biochars. This correlation is in agreement with the literature. Moreover, some of the catalytic oxides e.g. CaO, MgO present in the ashes of the PL biochars are refractory oxides and were reported to be good insulators due to their very low electrical conductivities, as mentioned earlier in this chapter.

Table 4.6: Electrical conductivity evolution with temperature for calcite, Arcanite, magnezite, silicon, and charcoal.

Temperature (° C)	Electrical conductivity (10^{-8} S/cm)				
	CaCO3 (Mirwald, 1979)	K2SO4 (Choi et al., 1993)	MgCO3 (Mibe and Ono, 2011)	SiO2 (Henry, 1924)	Charcoal (Antal and Gronli, 2003)
500	28	1160	0.001	8.8	0.33
600	70.7	17000	0.019	42	333
700	280	82200	0.199	130	333000

Compared to the electrical conductivities of industrial carbons e.g. graphite (10.50 S/cm) and activated carbon (0.80 S/cm) (Li et al., 2008), the PL biochars conductivities are so low that they were considered negligible. These very low electrical conductivities were a consequence of the high ash contents of the PL biochars.

4.5 Textural properties of the carbon fuels

The surface area of the carbon fuel is known to have a critical influence on the performance of the DCFC, since a high surface area would increase the interaction surface between the carbon fuel and the electrolyte. The S_{BET} surface area as well as the calculated total pore volume (V_p) of the three PL biochars are reported in Table 4.7. The total surface area and pore volume of the Black, Brown, and Tunisian biochars were 4.2 m^2/g, 3.88 m^2/g, and 3.34 m^2/g, respectively. As expected, the surface areas were very low compared to charcoal surface area which ranges from 330 m^2/g for *Cryptomeria Japonica* Charcoal (Iyobe et al.,

2004) to 360 m²/g for Bamboo charcoal (Asada et al., 2002). The low surface area of the PL biochars was due to the high amount of inorganics (oxides, salts, etc) in the three biochars. These inorganics are naturally incorporated in the biochar's skeleton, and they occupy the majority of pores and the external surface area of the three samples.

The pore volumes of the Black, Brown, and Tunisian biochars ($17.25x10^{-4}$ cm^3/g, $12.87x10^{-4}$ cm^3/g, and $18.39x10^{-4}$ cm^3/g, respectively) were very low compared to those of charcoals (~$0.18cm^3/g$) reported in the literature (Iyobe et al., 2004; Diaz-Taran et al., 2001). This was due to the high inorganic contents of the three PL biochars as explained for the low surface area. Compared to the surface area of industrial carbons e.g. activated carbon and graphitic carbon (1241-1305 m²/g and 39m²/g, respectively) (Li et al., 2008), the very low surface areas of the three biochars would decrease the performance of DCFC due to their small interaction-surface available to react with the electrolyte.

Interestingly, the surface area measurements of the PL biochars were very close to those of the coal samples (Table 4.7) reported in the literature i.e. GK and BW **(Li et al, 2010)**, however, the average pore volume of the poultry litter biochars was 5 times less than the average pore volume of the coal samples (GK and BW) probably because of the high ash content of PL biochars (32.5 and 47wt% for Tunisian and Black biochars, respectively) compared to the coal samples (5.8 and 6.4wt% for GK and BW, respectively). The similarity in surface area and the difference in pore volumes confirm the occupancy of the pores in PL biochars by the inorganic compounds.

Table 4.7: Textural properties, ash content, and carbon content of the different poultry litter biochars.

	C (wt%)	Ash (wt%)	S_{BET} (m^2/g)	V_p (cm^3/g)
Black	37.6	47	4.2±0.05	$17.25x10^{-4}$
Brown	22.8	63	3.88±0.02	$12.87x10^{-4}$
Tunisian	45.2	32.5	3.34±0.02	$18.39x10^{-4}$
Cryptomeria Japonica Charcoal[a]	-	-	330.2	0.18
Bamboo Charcoal[b]	-	-	175	0.12
Activated carbon[c]	90.8	<2	1241	0.55
Carbon black[c]	97.9	<2	118	0.28
Graphitic carbon[c]	98.2	<2	39	0.08
Coal GK[d]	-	5.8	7.9	0.013
Coal BW[d]	-	6.4	4.6	0.009

a: Iyobe et al., 2004
b: Asada et al., 2002
c: Li et al. 2008.
d: Li et al. 2010.

4.6 Chemical reactivity of the biochars

The temperature programmed oxidation (TPO) is employed to investigate the relative carbon oxidation i.e. the stability of the biochar in an oxidative atmosphere. A highly reactive carbon fuel will be beneficial for the performance of the DCFC since the discharge rate of the carbon particles at the anode would be higher. The TPO profiles for the three biochars are shown in Figure 4.4 a-b-c. A small weight loss at temperatures below 100° C corresponded to desorption of the physisorbed water (Li et al., 2008). The major weight losses for the three biochars took place between 250 and 500° C and they occurred within two stages (1) the initial release and subsequent ignition of volatiles followed by (2) transfer of the heat generated to the whole mass of the sample, initiating biochar combustion, respectively. The biochar combustion occurred at $T_{50\%}$ = 442.15° C, 436.6° C, and 437.5° C for the Black, Brown and Tunisian biochars and 44 wt%, 32 wt% and 60 wt%, respectively, of the sample's mass was burned-off.

The three biochars had higher oxidation reactivity compared to the industrial carbons, since their maximum oxidation rate occurs at an average temperature of 438.75° C (Figure 4.5) compared to an average of 630° C for the industrial carbons (Li et al, 2010). This high

reactivity of the PL biochars may be due to two factors (1) the high mineral matter (high ash content) in the biochars which can act as a catalyst of the oxidation of the carbon (Kirubakaran et al., 2007; Li et al., 2010b; Vuteutakis and Skidmore, 1987; Speight, 1994) and (2) the highly disordered structure of the biochars (Table 4.4) that led to a preponderance of edge sites and defects, which represent ideal reactive sites for the oxidation of carbon.

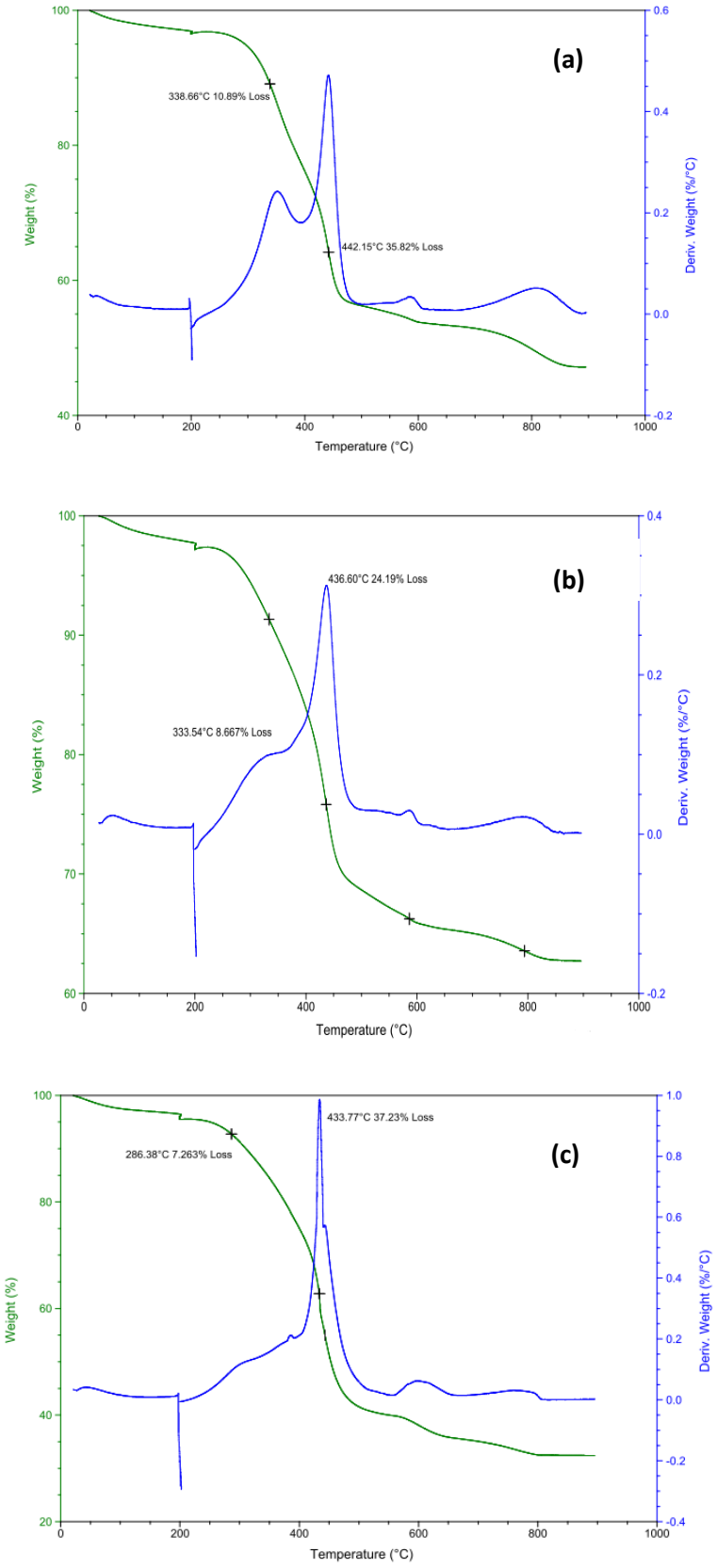

Figure 4.4: TPO profiles of (a) Black, (b) Brown, and (c) Tunisian biochar.

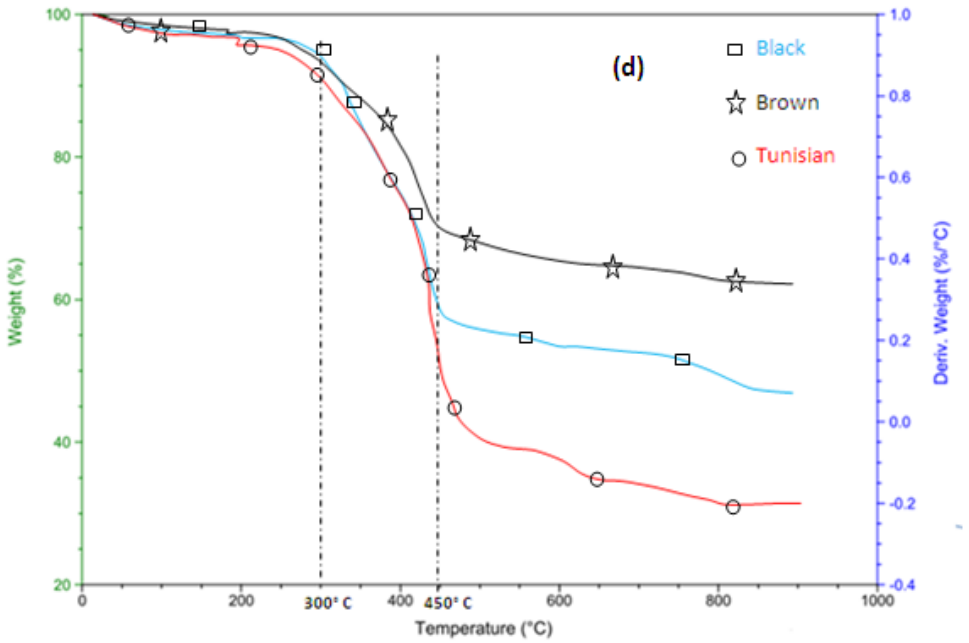

Figure 4.5: Overlaid TPO profiles of (▭) Black, (☆) Brown, and (○) Tunisian biochars.

4.7 Surface composition of the biochars

The surface composition of a carbon-rich material is very important for its electrochemical reactivity in fuel cells (Cao et al., 2010; Li et al., 2008; Li et al., 2010a). Temperature programmed desorption (TPD) is a common technique used to determine the nature and stability of the carbon surface oxygen complexes. The identification of the oxygen containing groups on the surface of the three biochars is possible through the measurement of the amount of carbon monoxide (CO) and carbon dioxide (CO_2) generated from the three biochars upon heating. The TPD profiles are very sensitive to the type of carbon used and the experimental conditions and this technique gives an approximate quantification of the oxygen-containing groups, but does not give enough information about the exact mechanism or the order of desorption of each oxygenated compound on the surface of the biochar. (Zhou et al., 2007; Räty J., 2001).

Figure 4.6 shows the temperature ranges of decomposition of the most common oxygen containing groups.

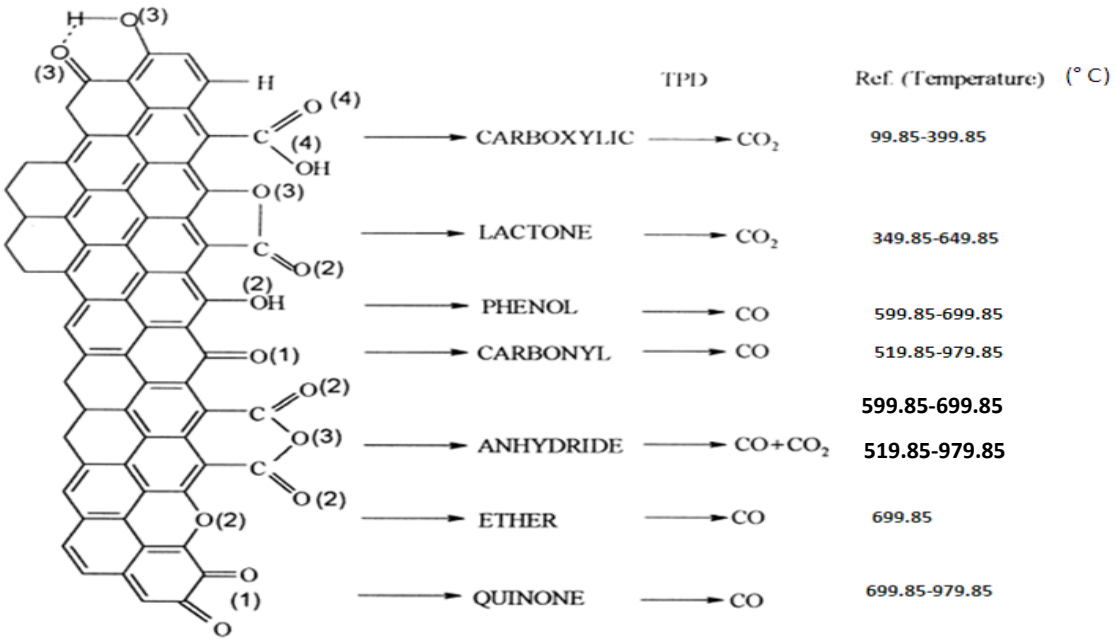

Figure 4.6: Common surface oxygen-containing groups and their decomposition temperatures. Figure modified from original. (Figueiredo et al.,1999).

In the CO_2 evolution profile (Figure 4.7-b), the Tunisian biochar generated the highest amount of CO_2 (0.18 mol% at $T_{50\%}$= 550° C) with a broad peak between 200 and 700° C and two smaller peaks at $T_{50\%}$ = 750° C (0.128 mol%) and 860° C (0.11 mol%). By contrast, the Black and Brown biochars have comparable low evolution of CO_2, which started slowly at 400° C and had two maximums at 770° C (0.048 mol%) and 840° C (0.085 mol%), respectively, but the latter produced slightly more CO_2 than the former. The low CO_2 evolution from the Black and Brown biochars was probably due to the fact that, they stayed in the hot gas filter (at 350-450° C) for at least 1 hour under nitrogen flow, thus the majority of the CO_2 yielding groups were destroyed/devolatilized and carried away from the biochars. However, the Tunisian biochar was not exposed to high temperatures for a long time, which explain the high CO_2 yielding groups. Particle size of the feedstock (poultry litter) was another factor behind the difference in CO_2 generation between the Tunisian and USA biomass (poultry litter). As mentioned in Chapter Three, the Tunisian poultry litter was pyrolysed as received (feedstock particles ~ 5 mm thick and 2mmx2mm surface area) while the USA poultry litter was ground to pass a 1-mm mesh screen. Large biomass particles Tunisian feedstock) will be under heat transfer limitation i.e. volatiles in the core of large particles will not be devolatilized completely during pyrolysis, thus the Tunisian poultry litter

was not pyrolysed completely, whereas the USA poultry litter was completely pyrolysed. This explanation was confirmed by the TGA analysis of the three PL biochars, where the Tunisian biochar generated more volatile matter than the USA biochars at temperatures under 550° C even if the pyrolysis temperature of the Tunisian poultry litter reached 600° C.

The CO_2 profile of the Tunisian biochar showed high similarity in shape with the CO_2 profile of the GK coal (Li et al., 2010b) with a broad peak at $T_{50\%}$= 500° C and a shoulder peak at $T_{50\%}$= 700° C. However, the CO_2 profiles of the commercial carbons (activated carbon, graphite, and carbon black) had different shapes compared to the Tunisian biochar. The similarity in CO_2 profiles between the coals and the Tunisian biochar was due to the temperature-unstable organic volatiles which were present in both of them. However, the industrial carbons had low organic volatiles content, which resulted in low CO_2 generation except for activated carbon which had a CO_2 peak at $T_{50\%}$=280° C which was due to the chemicals used during its activation.

The presence of calcium carbonate ($CaCO_3$) in the three biochars was confirmed by the CO_2 generation between 700 and 900° C due to the decomposition of $CaCO_3$ to CaO and CO_2.

In the CO evolution profiles (Figure 4.7-a), all three biochars presented a very low CO production (< 0.02 mol% for the three biochars) which is in disagreement with the literature where both CO and CO_2 evolved from the carbon materials during heating (Li et al., 2010b; Brewer et al., 2009; Li et al., 2008). The low evolution of CO for the three biochars was maybe due to the calibration of the gas chromatograph used in the TPD analysis. By contrast, the industrial carbons showed generation of both CO and CO_2 at different temperatures, implying the presence of different oxygen-containing groups (Li et al., 2008).

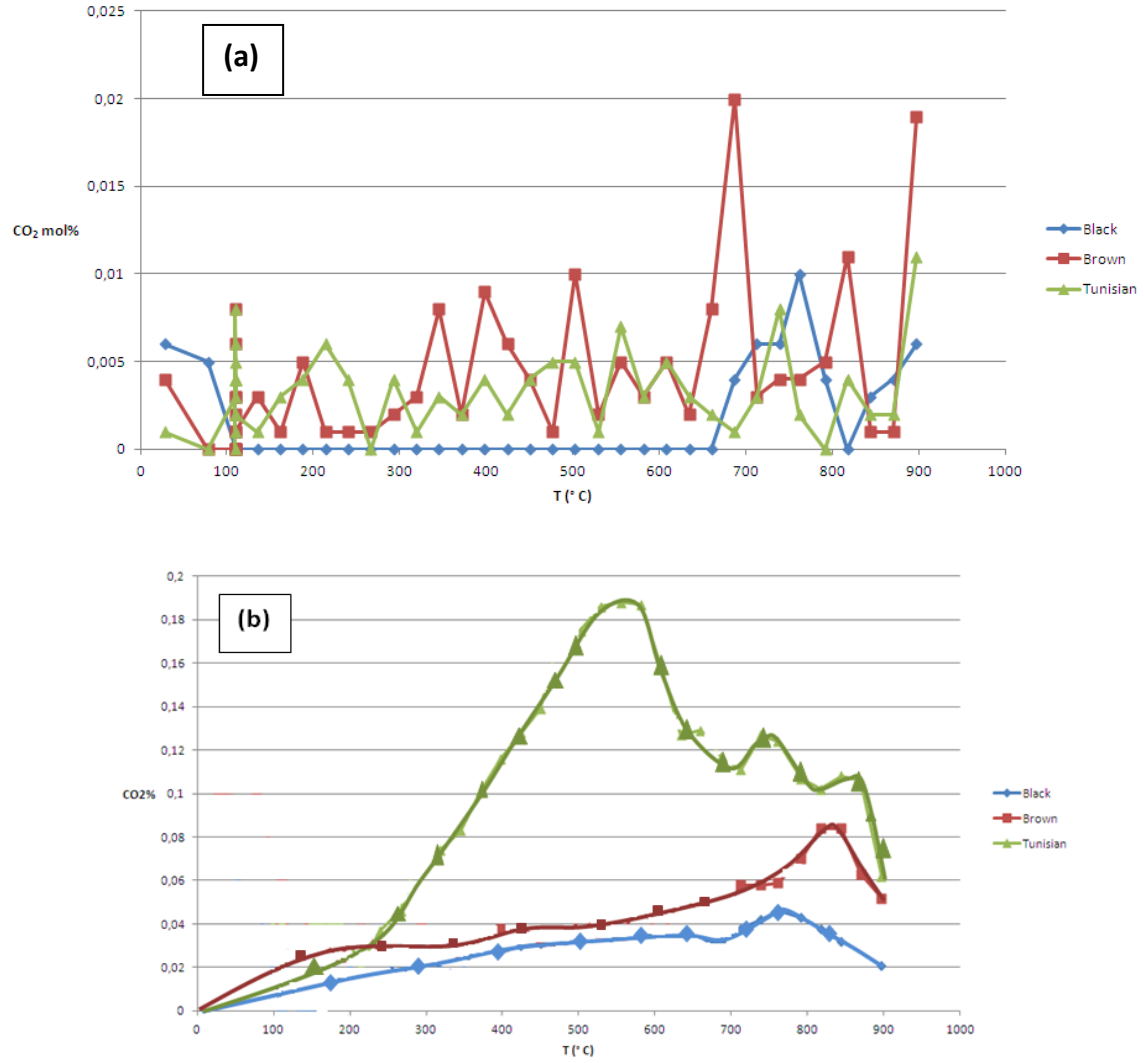

Figure 4.7 : (a) CO% and (b) CO_2% profiles for the Black, Brown, and Tunisian biochars.

4.8 Discussion

The characterization study of the poultry litter biochars i.e. Black, Brown and Tunisian revealed their physico-chemical properties. These properties are known to highly influence the performance of DCFC which would use these biochars as the anode fuel. The proximate analysis of the Black, Brown and Tunisian biochars showed that their fixed carbon content was low (22 wt%, 19 wt% and 35 wt%, respectively) which is not beneficial for the DCFC due to a low carbon loading. On the other hand, the ash contents were relatively high (47 wt%, 63 wt% and 32.5 wt%, respectively). As a consequence of the high ash content in the PL biochars, their surface areas were very low (less than 4.5 m^2/g for the three biochars)

compared to the industrial carbons (35 m^2/g for graphite and 1118 m^2/g for activated carbon) and charcoal (330.2 m^2/g) (Table 4.7). In fact, the oxides and salts occupied the majority of the porous structure of the biochars as well as their external surface area.

The ashes consisted on 3.21-6.62 wt% of minerals in the form of inhibitors (Al_2O_3 and SiO_2) for the anode reaction (Vutetakis and Skidmore 1987), and 40.24-43.08 wt% of minerals on the form of catalytic oxides (CaO, K_2O, MgO, Na_2O and Fe_2O) for the oxidation of the carbon (Li, 2008; Marsh and Reinoso, 2005), however these active catalysts have very low electrical conductivities (Wilson, 1981), which was confirmed by the low electrical conductivities of the Black, Brown and Tunisian biochars (70.56 nS/cm, 12.15 nS/cm and 7.7 nS/cm, respectively).

The low electrical conductivities of the biochars are not beneficial for the anodic reaction due to the high ohmic polarization which will decrease the DCFC performance (Li et al., 2008). Another cause of the very low electrical conductivities of the PL biochars was their highly disordered structure as shown by the XRD analyses (Table 4.4). Therefore, the electrical conductivity of the PL biochars is dependent on two parameters (1) the nature and concentration of mineral compounds in the ash of the carbonaceous material, (2) the degree of the structural disorder of the carbon material i.e. the lower graphitic structure a material has, the lower its electrical conductivity will be. However, the highly disordered structure of the PL biochars would enhance their electrochemical reactivity due to the preponderance of edge sites and defects, which increase the number of reactive sites for the carbon-electrolyte interactions, leading to a better performance of the DCFC.

The high reactivity of the biochar was proved by the TPO analyses which show that the PL biochars have a low average optimal burn-off temperature of 438.75° C versus 625° C for the industrial carbons (Li et al., 2008). In addition to the highly disordered structure, the high amount (40.24-43.08 wt%) of catalytic oxides in the PL biochars was behind the high oxidation reactivity of the PL biochars.

For such a low optimal-oxidation temperature, a special mixture of carbonates with a low melting point (< 400° C) must be used. Kouchachvili and Ikura (2011) reported that the addition of 20 wt% $CsCO_3$ to the ternary mixture (43.5 mol% Li2CO_3, 31.5 mol% Na_2CO_3, 25 mol% K_2CO_3) resulted in a low melting point (374° C) carbonate mixture. Such a mixture will be a suitable electrolyte for a DCFC using PL biochars as the anode fuel. However, and in addition to the low carbon loading, the use of PL biochars as anode fuels would result in a

dropping of the DCFC performance due to the high ash content of these biochars which will cause mass transfer limitation within the electrolyte (e.g. molten carbonates). In fact, the molten carbonates electrolyte is continuously stirred to ensure effective mass transfer of carbon particles between the electrolyte and the anode. The increasing percentage of the stable oxides (e.g. CaO, MgO, Na_2O, K_2O and Fe_2O_3), coming from the PL biochars, in the electrolyte would reduce the probability of contact between carbon particles and the anode.

Among the three biochars, the Tunisian one had the highest fixed carbon content (35 wt%) and the lowest ash content (32.5 wt%) as shown in Table 4.1. However, the carbon concentration of the Tunisian biochar is low compared to the industrial carbons (e.g. activated carbon: 90.8 wt% and graphitic carbon: 98.2 wt%) and coals (70.4 to 87.5 wt%). Low carbon content is not beneficial for the DCFC due to the low carbon loading which implies low discharge rate of the carbon on the anode compartment. Furthermore, despite the fact that the ashes of PL biochars contain mainly catalytic minerals (i.e. CaO, MgO, K_2O, Na_2O and Fe_2O_3), they still account for a high percentage of the PL biochars. The high ash content can cause inhibition of the anode reaction due to the very low electrical conductivity of these ashes as explained previously.

Therefore, the poultry litter biochars, as they are, cannot be used as anode fuels for DCFC. Further improvements of the properties (carbon content, electrical conductivity, surface area, etc) of the PL biochars are needed in order to make of them potential fuels for DCFC.

References

1. Alfieri, F., Gunning, P. J., Gallo, M., Del Borghi, A., Hills, C. D. 2012. Monitoring of carbon dioxide uptake in accelerated carbonation processes applied to air pollution control residues. *Presented at 25th conference Efficiency. cost. optimization. simulation and environmental impact of energy systems*. Perugia. ITALY. Proceeding of ECOS 2012.

2. Asada, T., Ishihara, S., Yamane, T., Toba, A., Yamada, A., Oikawa, K. 2002. Science of bamboo charcoal: study on carbonizing temperature of bamboo charcoal and removal capability of harmful gases. *Journal of health science.* 48: 473-479.

3. Bankauskaite, A., Baltakys, K. 2011. The Hydrothermal Synthesis of Hydrotalcite by Using Different Partially Soluble and Insoluble in Water Mangesium and Aluminium Components. *Sience of Sintering.* 43: 261-275.

4. Belgacem, K., Lewellyn, P., Nahdi, K., Ayadi, M. T. 2008. Thermal behaviour study of the talc. *Opteoelectronics and advanced materials.* 2: 332-336.

5. Brewer, C. E., Schmidt-Rohr, K., Satrio, J. A., Brown, R. C. 2009. Characterization of biochar from fast pyrolysis and gasification systems. *Environmental Progress & Sustainable Energy.* 28: 386-396.

6. Cao, D., Wang, G., Wang, C., Wang, J., Lu, T. 2010. Enhancement of electrooxidation activity of activated carbon for direct carbon fuel cell. *International Journal of hydrogen energy* 35: 1778-1782.

7. De Vries, K. J., Gellings, P.J. 1969. The thermal decomposition of potassium and sodium-pyrosulfate. *J. Inorg. Nucl. Chem.* 31: 1307-1313.

8. Diaz-Taran, J., Nevskaia, D. M., Lopez-Peinado, A. J., Jerez, A. 2001. Porosity and adsorption properties of an activated charcoal. *Colloids and Surfaces.* 187: 167-175.

9. Figueiredo, J. L., Pereira, M. F. R., Freitas, M. M. A., Orfao, J. J. M. 1999. Modification of the surface chemistry of activated carbons. *Carbon* 37: 1379-1389.

10. Gatternig, B., Hohenwarter, U., Schröttner, H., Karl, J. 2010. The influence of volatile alkali species on coating formation in biomass fired fluidized beds. *18th European Biomass Conference and Exhibition*. Austria.

11. Geisinger, K. L., Ross, N. L., McMillan, P., Navrotsky, A. 1987. K2Si4O9: Energetics and vibrational spectra of glasso sheet silicate. and wadeite-type phases. *American Mineralogist* 72: 984-994.

12. Iyobe, T., Asada, T., KAwata, K., Oikawa, K. 2004. Comparison of removal efficiencies for ammonia and amine gases between woody charcoal and activated carbon. *Journal of health science.* 50: 148-153.

13. Joseph, S. D., Downie, A., Munroe, P., Crosky, A., Lehmann, J. 2007. Biochar for Carbon Sequestration. Reduction of Greenhouse Gas Emissions and Enhancement of Soil Fertility; A Review of the Materials Science. *Proceedings of the Australian Combustion Symposium* University of Sydney.

14. Jung, C., Bobet, A., Siddiki, N. Z. 2011. Simple Method to Identify Marl Soils. *Transportation Research Record.* 2232: 76-84.

15. Khan, N., Dollimore, D., Alexander, K., Wilburn, F.W. 2000. The origin of the exothermic peak in the thermal decomposition of basic magnesium carbonate. *Thermochemica Acta.* 367: 321-333.

16. Kirubakaran, V., Sivaramakrishnan, V., Premalatha, M., Subramanian, P. 2007. Kinetics of auto-gasification of poultry litter. *International Journal of Green Energy* 4: 519-534.

17. Kouchavichvili, L., Ikura, M. 2011. Performance of direct carbon fuel cell. *International Journal of Hydrogen Energy.* 36: 10263-10268.

18. Li, X. 2008. "Tailoring carbon materials as fuels for the direct carbon fuel cells". PhD thesis (University of Queensland, Australia).

19. Li, X., Zhu, Z., De Marco, R., Bradley, J., Dicks, A. 2010a. Modification of Coal as a Fuel for the Direct Carbon Fuel Cell. *Journal of physical chemistry* 114: 3855-3862.

20. Li, X., Zhu, Z. H., De Marco, R. Dicks, A., Bradley, J., Liu, S., Lu, G. Q. 2008. Factors That Determine the Performance of Carbon Fuels in the Direct Carbon Fuel Cell. *Industrial and engineering chemistry research* 47: 9670-9677.

21. Li, X., Zhu, Z., De Marco, R., Bradley, J., Dicks, A. 2010b. Evaluation of raw coals as fuels for direct carbon fuel cells. *Journal of Power Sources* 195: 4051-4058.

22. Lin, Q., Guet, J. M. 1990. Characterization of coal and macerais by X-ray diffraction. *Fuel.* 69: 821-825.

23. Lu, L., Sahajwalla, V., Kong, C., Harris D. 2001. Quantitative X-ray diffraction analysis and its application to various coals. *Carbon.* 39: 1821-1833.

24. Manoj, B., Kunjomona, A. G. 2012. Study of Stacking Structure of Amorphous Carbon by X-Ray Diffraction Technique. *International Journal of Electrochemical Science* 7: 3127-3134.

25. Mante, O. D., Agblevor, A. F. 2010. Influence of pine wood shavings on the pyrolysis of poultry litter. *Waste Management.* 30: 2537-2547.

26. March, H., Rodriguez-Reinoso, F. 2005. "Activated carbon," 1st edition. Elsevier Science., San Diego, California.

27. Marinov, S. P., Gonsalvesh, L., Stefanova, M., Yperman, J., Carleer, R., Reggers, G., Yürüm, Y., Groudeva, V., Gadjanov, P. 2010. Combustion behaviour of some biodesulphurized coals assessed by TGA/DTA. *Thermochemica Acta* 497: 46-51.

28. Räty, J., Pakkanen, T. A. 2001. Temperature-programmed desorption study of Re/ gamma -Al 2 O 3 catalysts prepared from Re 2 (CO) 10 precursor. *Applied Catalysis A: General* 208: 169-175.

29. Skreiberg, A., Skreiberg, O., Sandquist, J., Sorum, L. 2011. TGA and macro-TGA characterisation of biomass fuels and fuel mixtures. *Fuel* 90: 2182-2197.

30. Som Phytopharma INDIA Ltd., INDIA: http://www.somphyto.com/probiotics_poultry_littermanage.htm

31. Speight, J. G. 1994. "The chemistry and technology of coal", 2nd edition. Marcel Dekker Inc. New York.

32. Varhegyi, G., Szabo, P. 2002. Kinetics of charcoal devolatilization. *Energy & Fuels.* 16: 724-731.

33. Vutetakis, D.G., Skidmore, D. R., Byker, H.G. 1987. Electrochemical oxidation of molten carbonate-coal slurries. *J. Electrochem. Soc.* 134: 3027-3035.

34. Wang, C., Zhao, J., Zhao, X., Bala, H., Wong, Z. 2006. Synthesis of nanosized calcium carbonate (aragonite) via a polyacrylamide inducing process. *Powder Technology.* 163: 134-138.

35. West, A. R. 1999. "Basic Solid State Chemistry," 2nd edition. John Wiley & Sons Ltd., Chichester, England.

36. Wei, H., Shen, Q., Zhao, Y., Wang, D. J., Xu, D. F. 2003. Influence of polyvinylpyrrolidone on the precipitation of calcium carbonate and on the transformation of vaterite to calcite. *Journal of Crystal Growth.* 250: 516-524.

37. Wilson, I.O. 1981. Magnesium oxide as a high-temperature insulant. *IEE Proceedings A Physical Science, Measurement and Instrumentation, Management and Education, Reviews.* 128: 159-164.

38. Zhou, J. H., Sui, Z. J., Zhu, J., Li, P., Chen, D., Dai, Y. C., Yuan, W. K. 2007. Characterization of surface oxygen complexes on carbon nanofibers by TPD. XPS and FT-IR. *Carbon* 45: 785-796.

Chapter 5
Improvement of the electrochemical properties of the biochars

Abstract

The low fixed carbon contents, the negligible electrical conductivities and the low surface areas of the poultry litter (PL) biochars were behind its bad classification as anode fuel for DCFC. Interestingly, the bad properties of the three biochars were a result of their high ash contents. In order to improve upon these properties (electrical conductivity, carbon content, surface area) of the poultry litter biochars, different demineralization techniques were suggested i.e. physical, chemical and biological demineralization. Chemical demineralization of poultry litter biochars was qualified as the most efficient demineralization technique with a high potential of being applied in the industrial scale, if appropriate recycling and recovery techniques are applied to the demineralization process. As a consequence of the demineralization in the sequence HF/HCl, PL biochars would still contain calcium (in the form of CaF_2), which is a catalyst for the carbon oxidation reaction, their surface areas and surface oxygen-containing functional groups are expected to increase as well as their fixed carbon contents. A carbonization treatment (at 950° C) of the three biochars, after demineralization, would further increase their fixed carbon contents as well as their electrical conductivities, but at the same time the carbonization treatment of PL biochars would decrease their surface oxygen-containing functional groups, which may lower the performance of the DCFC.

Chemical demineralization of the PL biochars followed by carbonization at high temperatures would reduce the ash content, increase the surface area, increase the fixed carbon content, and increase the electrical conductivities of the three biochars. With such properties, the Black, Brown and Tunisian biochars would be qualified as potential anode for DCFC.

5.1 Introduction

After the characterization study of the poultry litter biochars (Chapter 4) it was clear that they cannot be considered as a potential fuel for DCFC due to their low fixed carbon content (less than 36 wt%) and very low electrical conductivity (less than 71 nS/cm) which was partly related to their disordered structure and mainly to their high ash content (32.5-63 wt%). However, the ash of PL biochars contained around 40 wt% of catalytic oxides for the carbon oxidation reaction, and around 5 wt% inhibitory oxides for the anode reaction. Therefore, the ash of PL biochar can be considered as catalytic ash.

Therefore, there is a need for methods and feasible techniques to improve the electrochemical properties of those biochars in order to use them as anode fuel in DCFC. These techniques should minimize the side effects of the ashes mentioned earlier in this paragraph. In this chapter, different feasible solutions will be proposed to improve upon the electrochemical properties of the PL biochar.

5.2 Properties improvement of the PL biochars

5.2.1 Demineralization of the PL biochars

As mentioned before, the high ash content in the PL biochars was behind their very low electrical conductivities since the literature reported a high electrical conductivity i.e. $1.51x10^{-4}$ S/cm for charcoals prepared at 650° C, with less than 5 wt% ash (Mochidzuki et al., 2003). Therefore, the demineralization of the biochars is necessary in order to improve upon their electrical conductivities. Weaver et al. (1975) reported that ash content up to 10 wt% in coal didn't have a measurable change in the polarization curves of a molten carbonate fuel cell. Thus it can be assumed that 10 wt% ash in the carbon fuel for DCFC is a critical value above which measurable drops in the polarization curves may occur. To bring the ash content of the three biochars to less than 10 wt%, several demineralization techniques, discussed in the literature, can be used; physical separation, chemical separation and biological separation.

5.2.1.1 Physical demineralization

Physical demineralization of carbonaceous materials is based on the density difference between char particles and the minerals in the carbonaceous material. Dyrkacz and Horwitz

(1980) described the physical demineralization of coal as follows; the carbon sample is ground to very fine particles, typically 3-5 µm median size, to separate the organics from the inorganics. Later, the fine carbon powder is suspended in a solution containing a surfactant (e.g. CsCl), which will reduce the surface tension between the solids and the surrounding solution, allowing better wet-ability of the carbon particles. The mixture is then dispersed with a high speed mixing. Finally, the mixture is centrifuged at high centrifugal force (e.g. 30000 g) and the carbon material is siphoned off with the float layer. This process would reduce the minerals content by only 27 wt%, which is not enough to bring the ash content of the poultry litter biochars to 10 wt%.

5.2.1.2 Chemical demineralization

The chemical demineralization of carbon materials consists on dissolving the water-and acid-soluble parts of the mineral matter present in the sample, and the conversion of the water-insoluble portion into soluble parts using the oxidative effect of some solvents (e.g NaOH, HNO_3, etc). The high efficiency of the chemical demineralization is due to the selective leaching of inorganic constituents by various solvents. Combination of different solvents (e.g. HF/HCl and HF/HNO_3) had been investigated in the literature, and proved higher demineralization efficiency than the single solvent process (Kizgut et al., 2006; Ishihara et al., 2004). The most frequent chemical separation process used for coal cleaning is the use of dilute alkali followed by washing with acids (Bolat et al., 1998). The solvents used in chemical demineralization processes are various inorganic acids such as HF, HCL, HNO_3 and H_2SO_4 (Steel and Patrick, 2001).

For high ash content coals (44-69 wt%), Bolat et al. (1998) reported that the use of minerals extraction with 0.5 mol/L of NaOH followed by leaching with 10% HCl resulted in the maximum degree of demineralization i.e. 46.78%. However, for poultry litter biochars, the presence of calcium is necessary since it plays a dominant catalytic role during the char oxidation (Zhang et al., 2010). Therefore, the order of acid washing of PL chars is very important in order to keep the calcium from being removed with the other minerals. In fact, the optimal demineralization process was reported in the following sequence; leaching the samples for 2 hours in 4800 ml of 3% HF solution, followed by leaching for 2 hours in 4800 ml of 5M HCL solution. Such a process removed nearly all minerals except calcium which was fully recovered in the form of CaF_2 (stable and insoluble compound). That is due to the fact that during HF acid treatment, CaF_2 is formed, then the HCl acid washing removed nearly all minerals.

5.2.1.3 Biological demineralization

Bioleaching was another technique for demineralization of carbonaceous materials with high ash content. It consists of using micro-organisms to reduce the mineral content of the sample through different mechanism; biooxidation, bioreduction, acidification and ligand production. In these mechanisms, the metals present in the ash of the carbon material are transformed indirectly by reaction with cellular metabolites or directly as a part of the cell's energy generation or metal detoxification (Olson and Kelly, 1986; Hutchins et al., 1986). Using bioleaching for the demineralization of high ash content coals was carried by Sharma and Wadhwa (1997) as follows; 10 grams of sterilized coal were dispersed in distilled water. Inoculum culture was added at 10 vol%, after adjusting the volume to 100 ml with distilled water, incubation at 37° C was carried for 7 days. Residual coal was centrifuged and washed thoroughly, then dried at 105° C for 3 hours in a vacuum oven then cooled in a dessicator before analysis. The mineral matter was reduced by 50%. However, the demineralization yield was highly dependent on the reaction parameters i.e. pH, inoculum size, incubation temperature and the culture medium. In addition to that, the reaction time was long (7 days).

5.2.2 Carbonization of the PL biochars

Carbonization of carbonaceous material is well known to increase their fixed carbon content (due to the devolatilization of the volatile matter) as well as their electrical conductivities. These two properties are very important for the anode fuel of a DCFC. Morchidzuki et al. (2003) reported that carbonization of charcoal at 950° C under nitrogen atmosphere (1L/min), resulted in graphitelike electrical properties without any changes in its crystalline structure. The electrical conductivity of the carbonized charcoal was 9.1 S/cm. Therefore, they visualized carbonized charcoal as a macromolecular, cross-linked, three dimensional, aromatic structures with conjugation and π bonds that facilitate the conduction of electrons. The high fixed carbon content results in a high carbon loading, which would increase the carbon discharge in the anode. The high electrical conductivity would result in a low ohmic polarization, thus the improvement of the anode reaction (Li et al., 2008). Therefore, the carbonization of the poultry litter is believed to increase their carbon contents and improve their electrical conductivities. However, the fixed carbon content of the carbonized PL biochars will never be as high as in the industrial carbons (activated carbon, carbon black, and graphitic carbon) or coals, and that is due to the high ash content in PL biochars which can't be removed by carbonization. Furthermore, carbonization at high temperature would

destroy the oxygen-containing functional groups in the PL biochars. In fact, at 650° C, O-H groups, the aliphatic C-H groups and in a great part the C=O groups decompose. The absence of these oxygen-groups would decrease the reactivity of the poultry litter biochars, since the presence of these groups would provide more reactive sites in the PL biochars, thus enhance the discharge rate of the carbon in the DCFC (Cooper et al., 2005). Further investigation of the treated PL biochar is needed.

5.3 Discussion

Physical separation can reduce the amount of mineral matter in heterogeneous carbon materials, however, this technique may not be efficient when mineral grains are tiny and strongly bound to the surrounding carbonaceous material. The biological separation was claimed to reduce the mineral matter content up to 50 wt%, however, this process have some disadvantages i.e. the long reaction time (7 days) and of the high dependence of the micro-organism's activity on reaction parameters such as pH, incubation temperature, and the inoculum size, which mean that continuous control of the reaction vessel is needed. Chemical demineralization is known as being the only solution to obtain clean demineralised carbons, which explain its extensive use in the production of ultra clean coal (UCC). In addition, the use of oxidative chemicals during the chemical demineralization, increase the number of the surface oxygen-containing functional groups in the PL biochars, which will improve their reactivity in DCFC (Li et al., 2008). In addition to that, chemical demineralisation can be selective, which allow the conservation of some minerals over the undesired ones (Zhang et al., 2010). However, chemical processes are likely to be more expansive than physical processes in terms of both capital and operating cost. Therefore, the development of efficient method for the recovery and recycling of the chemicals used in the demineralization process would reduce remarkably its cost and make it the most suitable and efficient demineralization process for heterogeneous carbonaceous materials.

After reducing the mineral matter content of PL biochars to less than 10 wt%, which is the critical ash content that can affect the anode reaction (Weaver et al., 1975), it is possible to estimate the DCFC operation time T_c before which, inhibition of the anode reaction will occur. Assuming an ash fraction "f" in the demineralised PL biochars, the theoretical time T_c to reach the critical ash concentration (10 wt% i.e. fraction f_c=0.1) for a typical salt loading W_{el}~ 2.3 g/cm² under a fuel cell current density of i= 0.1 A/cm² is:

$$T_c = \frac{f_c n F W_{el}}{i M_c f}$$

M_c is the atomic weight of carbon and F is the Faraday constant. This criterion suggests a useful lifetime of the melt of at least T_c (days) ~ $0.86/f$. Thus, if we consider a demineralised PL biochars with an ash content of 5 wt%, the critical time T_c would be 17 days.

The elimination of minerals from the poultry litter will unblock the pores and "clean" the external surface of the material, thus a higher surface area and pore volume are expected for the demineralised PL biochars, which is beneficial for their reactivity on DCFC since higher surface area and pore volume means higher reaction interface between the carbon and electrolyte. Furthermore, after demineralization, poultry litter biochars will have a similar chemical composition to that of charcoal. Interestingly, the electrical conductivity of charcoal is highly dependent on its precursor and its preparation condition. The electrical conductivity and the fixed carbon content of charcoal can vary from $1.5x10^{-4}$ S/cm and 87.9 wt% (when carbonized at 650° C) to 16.94 S/cm and 95.13 wt% (when carbonized at 1050° C), respectively (Mochidzuki et al., 2003). Therefore, the carbonization of the demineralised poultry litter biochars should increase more their electrical conductivity as well as their fixed carbon content.

As a result of the chemical demineralization followed by carbonization, poultry litter biochars will have higher fixed carbon content, (which means higher carbon loading in the DCFC), higher surface area (which means higher reaction interface for the carbon-electrolyte interaction), and higher electrical conductivities (which would lower the ohmic polarization of the anode). Moreover, the treated PL biochars would contain a potential catalyst (calcium in the form of CaF_2) for carbon oxidation. All these three criteria would improve the performance of DCFC.

References

1. Bolat, E., Saglam, S., Piskin, S. 1998. Chemical demineralization of a Turkish high ash bituminous coal. *Fuel Processing Technology.* 57: 93-99.

2. Cooper, N. J. Krueger, R., Fiet, K. J., Jankowski, A. F., Cooper, J. F. 2005. Direct conversion of carbon fuels in a molten carbonate fuel cell. *Journal of the electrochemical society.* 152: A80-A87.

3. Dyrkacz G. R., Horwitz, E. P. 1982. Separation of coal macerals. *Fuel.* 61: 3-12.

4. Hutchins, S.R., Davidson, M. S., Brierley, J. A., Brierley, C. L. 1986. Microorganisms in reclamation of metals. *Annual Review in Microbiology* 40: 311-336.

5. Ishihara, A., Sutrisna, I. P., Finahari, I., Qian, E. W., Kabe, T. 2004. Effect of demineralization on hydrogen transfer of coal with tritiated gaseous hydrogen. *Fuel Processing Technology.* 85: 887-901.

6. Kizgut, S., Baris, K., Yilmaz, S. 2006. Effect of chemical demineralization on thermal behaviour of Bituminous coals. *Journal of Thermal Analysis and Calorimetry.* 86: 483-488.

7. Li, X. 2008. "Tailoring Carbon Materials as Fuels for the Direct Carbon Fuel Cells". PhD thesis (University of Queensland, Australia).

8. Mochidzuki, K., Soutric, F., Tadokoro, K., Antal, M. J. Toth, M., Zelei, B., Varhegyi, G. 2003. Electrical and physical properties of carbonized charcoals. *Ind. Eng. Chem. Res.* 42: 5140-5151.

9. Olson, G. J., Kelly, R. M. 1986. Microbiological metal transformations: biotechnological applications and potential. *Biotechnology Progress* 2: 1-15.

10. Sharma, D. K., Wadhwa, G. 1997. Demineralization of coal by stepwise bioleaching: a comparative study of three Indian coals by Fourier Transform Infra Red and X-ray diffraction techniques. *World Journal of Microbiology & Biotechnology.* 13: 29-36.

11. Steel, K. M., Patrick, J. W. 2001. The production of ultra clean coal by sequential leaching with HF followed by HNO_3. *Fuel.* 82: 1917-1920.

12. Weaver, R. D., Tietz, L., Cubicciotti, D. 1975. Direct use of coal in a fuel cell: Feasibility Investigation. EPA-650/2-75-040, June.

13. Zhang, S. Y., Cao, J. P., Takarada, T. 2010. Effect of pretreatment with different washing methods on the reactivity of manure char. *Bioresource Technology*. 101: 6130-6135.

General conclusions

- Poultry litter biochars are not potential anode fuels for DCFC due to their low fixed carbon contents and high ash contents. The low fixed carbon content would cause low carbon loading in the DCFC and the high ash content would result in low surface area, thus a low carbon-electrolyte reaction interface. Furthermore the high ash content would result in a high ohmic polarization of the anode in DCFC.

- The high oxidation reactivity of PL biochars was due to their ashes that contain around 40 wt% alkali and alkaline earth metal oxides (CaO, MgO, K_2O, Na_2O, and Fe_2O_3). These oxides were reported in the literature as catalysts (especially calcium based oxides) for the oxidation reaction of carbon.

- Demineralization of the poultry litter biochars in the sequence HF/HCl would keep the calcium in the form CaF_2 in the biochars and would increase their fixed carbon content and increase their surface area by washing away the mineral matter except calcium. Additional carbonization of the demineralised PL biochars at 950° C would further increase their surface areas and increase their electrical conductivities. Consequently, the treated PL biochars would be potential fuels for DCFCs.